

BEYOND NO_x: EMISSIONS OF UNREGULATED POLLUTANTS FROM A MODERN GASOLINE CAR

Felipe Rodríguez and Jan Dornoff

ACKNOWLEDGEMENTS

The authors thank the Joint Research Centre of the European Commission for conducting the vehicle tests, which were performed under collaborative research agreement No. 34216. The authors also thank all internal and external reviewers of this report for their guidance and constructive comments, with special thanks to the Joint Research Centre of the European Commission; Peter Mock, John German, Anup Bandivadekar, and Huzeifa Badshah (International Council on Clean Transportation), and Joseph Kubsh (Manufacturers of Emission Controls Association). Their review does not imply an endorsement, and any errors are the authors' own.

For additional information:
International Council on Clean Transportation Europe
Neue Promenade 6, 10178 Berlin
+49 (30) 847129-102

communications@theicct.org | www.theicct.org | [@TheICCT](https://twitter.com/TheICCT)

© 2019 International Council on Clean Transportation

Funding for this work was generously provided by the European Climate Foundation.

EXECUTIVE SUMMARY

To gain a better understanding of the pollutant emissions of modern gasoline vehicles, a 2018 Volkswagen Golf TSI was tested on the chassis dynamometer over the regulatory cycles, and over two real-world cycles. The vehicle was equipped with a gasoline direct injection engine and was compliant with the emissions norm Euro 6c. The tests were done at different ambient conditions and with a cold and warmed-up engine. The analysis focused on the emissions of both regulated and unregulated pollutants, with the following key findings:

1. **The vehicle exhibited good emissions performance for regulated pollutants.**
The emissions over all of the test runs were below the Euro 6 standards, with the exception of the cold-start tests at -7°C. Over these low temperature tests, the Euro 6 limits were exceeded for hydrocarbons (HC) and particulate number (PN).
2. **There were a substantial number of particles in the unregulated size range, from 10 to 23 nm.** If solid particles in this sub-23 nm range had been accounted for, the total emissions of solid PN would have been up to 114% higher. Accounting for volatile particles would further increase PN emissions by up to 78%.
3. **Ammonia emissions are comparable to the emissions of nitrogen oxides (NO_x).** Ammonia emissions are becoming a significant source of reactive nitrogen compound in gasoline exhaust. Ammonia emissions amounted to half the mass NO_x emissions and were 10% higher than the molar NO_x emissions.
4. **Methane and nitrous oxide, both powerful greenhouse gases, were found in non-negligible amounts in the exhaust gas.** Their combined effect accounted for up to 0.75% of the vehicle's greenhouse gas (GHG) footprint when using the 20-year global warming potential factors.
5. **Formaldehyde, a highly toxic substance, was found in non-negligible amounts in the exhaust gas.** Formaldehyde emissions were constrained to the cold-start test and were mostly emitted within the first minute of operation.

These findings contribute to the wealth of evidence on the emissions of unregulated pollutants. They point to the following policy recommendations for post-Euro 6 standards:

1. Extend the low temperature test (type 6 test) at -7°C to include all regulated pollutants, in particular PN.
2. Reduce the size threshold for solid particle counting from 23 nm to 10 nm and consider the inclusion of volatile particles in the measurement methodology.
3. Introduce technology- and application-neutral limits for vehicular ammonia emissions.
4. Establish technology- and application-neutral limits for methane and nitrous oxide emissions, or account for their CO₂-equivalent emissions in the CO₂ standards.
5. Introduce technology- and application-neutral limits for vehicular formaldehyde emissions. Formaldehyde emissions are already regulated in the United States.

TABLE OF CONTENTS

Executive summary	i
Abbreviations	iii
Introduction	1
Methodology	2
Test vehicle.....	2
Experimental setup and instrumentation.....	3
Tests conducted	4
Results and general discussion	6
Regulated pollutants	6
Ultrafine particulate emissions	7
Interim conclusion.....	12
Ammonia.....	12
Interim conclusion.....	15
Greenhouse gases	16
Interim conclusion.....	19
Aldehydes.....	19
Interim conclusion.....	21
Summary and policy recommendations	22
Policy recommendations	23
References	24
Appendix: Tabulated emissions	30

ABBREVIATIONS

CH ₄	methane
CO	carbon monoxide
CPC	condensation particle counter
CS	catalytic stripper
CVS	constant volume sampling
DAQ	data acquisition
E5	gasoline with 5% ethanol volume fraction
EEPS	Engine Exhaust Particle Sizer
ET	evaporation tube
FTIR	Fourier-transform infrared spectroscopy
FTP	Federal Test Procedure
GDI	gasoline direct injection
GPF	gasoline particulate filter
GWP	global warming potential
H ₂	hydrogen
HC	hydrocarbons
HCHO	formaldehyde
JRC	Joint Research Centre
MeCHO	acetaldehyde
N ₂ O	nitrous oxide
NEDC	New European Driving Cycle
NH ₃	ammonia
NH ₄ ⁺	ammonium ion
nm	nanometer
NMHC	non-methane hydrocarbons
NO	nitric oxide
NO ₃ ⁻	nitrate ion
NO _x	nitrogen oxides
PCRF	particle number concentration reduction factor
PM	particulate mass
PMP	Particle Measurement Programme
PN	particulate number
RDC	Real Driving Cycle
RDE	Real Driving Emissions
TWC	three-way catalyst
UNECE	United Nations Economic Commission for Europe
VELA	Vehicle Emission Laboratory
VPR	volatile particle remover
WLTC	Worldwide Harmonized Light-duty Test Cycle
µm	micrometer

INTRODUCTION

Motor-vehicle emissions and their link to air pollution have been recognized as a serious issue since the 1950s, when the link between combustion emissions and photochemical smog was established (Haagen-Smit, 1952). However, it was not until 1970 that the matter was addressed with regulatory action at the European level. Directive 70/220/EEC (Council of the European Union, 1970) established emissions limits for carbon monoxide (CO) and unburned hydrocarbons (HC) of gasoline-powered vehicles. The landmark directive was amended several times over the following decades to extend its scope: Emissions limits for nitrogen oxides (NO_x) were introduced in 1977,¹ amendments to also cover the gaseous pollutants of diesel vehicles were passed in 1983,² and a particulate mass (PM) emissions limit was introduced for diesel vehicles in 1988.³

In 1992, the introduction of what is known today as Euro 1⁴ marked a new regulatory era for pollution control. Since then, the European Union has moved quickly to further tighten emission limits.⁵ Still, the list of pollutants covered by the regulations has remained the same: CO, HC, NO_x, and particulates. The Euro 5 standards, however, introduced a new metric to limit the particulate emissions of diesel engines: the particle number (PN). The PN limits, which only cover solid particles larger than 23 nanometers (nm), were extended to also cover gasoline direct injection (GDI) engines under the Euro 6 standards.

As the emissions of most regulated pollutants continue to decrease as a result of the Euro standards, in particular for gasoline vehicles (Bernard, Tietge, German, & Muncrief, 2018), the emissions of unregulated pollutants become more relevant. Although the tailpipe concentrations of ultrafine particles smaller than 23 nm, ammonia, aldehydes, and cyanide compounds are lower than the concentration of regulated pollutants, their marked health and atmospheric impacts warrant a closer examination. Future emission standards should take into account the available evidence pertaining to these unregulated pollutants. The purpose of this study is to contribute to this body of knowledge.

This paper presents the results of chassis dynamometer testing of a Euro 6 GDI vehicle. The emissions over different driving cycles were measured, and a particular focus was placed on pollutants that are not currently regulated. The paper starts with a discussion of the test vehicle and the methodology. Then, for each unregulated pollutant considered, we present a summary of the available evidence and the results of the present study, and discuss the relationship of the experimental results with the literature. Closing the paper, we formulate a set of policy recommendations for the development of future emission standards.

The results of this testing project are not intended as a generalization of the emissions behavior of GDI vehicles, but must be interpreted as a case study highlighting areas where scientific consensus exists or where further research is recommended.

1 NO_x limits we introduced by Directive 77/102/EEC (European Commission, 1977).

2 CO, HC, and NO_x limits we introduced for compression ignition engines by Directive 83/351/EEC (Council of the European Union, 1983)

3 Directive 72/306/EEC (Council of the European Union, 1972) addressed black carbon emissions of diesel vehicles only through opacity measurements. Directive 88/436/EEC (Council of the European Union, 1988) introduced the direct measurement of the particulate mass.

4 Although Directive 91/441/EEC (Council of the European Union, 1991) is now known as Euro 1, the Euro nomenclature was first officially introduced in 2007.

5 Directive 96/69/EC (Parliament and Council of the European Union, 1996) defines the Euro 2 standards. Directive 98/69/EC (Parliament and Council of the European Union, 1998) defines the Euro 3 and Euro 4 limits. Regulation (EC) No 715/2007; (European Commission, 2007) establishes the Euro 5 and Euro 6 limits.

METHODOLOGY

A popular gasoline passenger vehicle of the C-segment, compliant with the emission standard Euro 6c, was tested at the facilities of the European Commission Joint Research Centre (JRC) in Ispra, Italy. This section presents the details of the test vehicle, the experimental setup and instrumentation, and the tests performed on the chassis dynamometer.

TEST VEHICLE

The test vehicle was a gasoline Volkswagen Golf 1.5 TSI ACT BlueMotion (see Figure 1). It had a mass in running order of circa 1,350 kg, was equipped with a 7-gear dual-clutch transmission, and was powered by a 1.5 liter, 4-cylinder engine with a rated power of 96 kW and a rated torque of 200 Nm.



Figure 1. Volkswagen Golf 1.5 TSI ACT BlueMotion on JRC's chassis dynamometer

The engine's GDI system featured a side-mounted, 5-hole fuel injector, with an injection pressure between 170 and 350 bar. The injection system was capable of up to five injections per cycle. The engine featured several fuel-saving technologies such as cylinder deactivation, active coolant temperature control, and controllable camshaft phasing on both the intake and exhaust valvetrains. The variable valve timing allows the engine to run in a more efficient part-load combustion mode, dubbed Miller cycle. While the Miller cycle increases the engine efficiency by reducing the throttling losses and increasing the expansion ratio, it also results in lower exhaust temperatures, which can negatively impact the conversion efficiency of the aftertreatment system. However, the lower exhaust temperatures allow the use of a variable geometry turbocharger, which provides an additional degree of freedom for emissions calibration. The vehicle also featured an advanced coasting mode, in which the wheels are decoupled from the engine during coasting phases.

The aftertreatment system consisted of a close coupled three-way catalyst (TWC), and a second underfloor TWC. The vehicle was compliant with the Euro 6 standard, stage c, and was not equipped with a gasoline particulate filter (GPF).⁶ At the beginning of the testing, the vehicle's odometer was close to 11,000 km. However, the original aftertreatment system was replaced with new parts during the vehicle instrumentation. The new catalysts were aged for approximately 1,500 km over a mix of urban, rural, highway, and mountain driving prior to testing. This distance was deemed sufficient to *degreen* the TWC. Catalyst degreening eliminates the possibility of the reduced catalytic activity typical of fresh converters.

⁶ The 2019 version of the Golf TSI, compliant with the Euro 6d-TEMP standard, does equip a GPF.

EXPERIMENTAL SETUP AND INSTRUMENTATION

The vehicle testing was performed in the Vehicle Emission Laboratory (VELA) at the JRC (Giechaskiel et al., 2007). The testing facility includes a four-wheel drive chassis dynamometer (roller diameter of 1.2 m) inside of a climatic test cell with controlled temperature and humidity. To simulate different ambient conditions, the temperature can be adjusted continuously between -10°C and 35°C.

The emissions of regulated gaseous pollutants were analyzed by a constant volume sampling (CVS) system with a critical flow venturi nozzle. The regulated pollutant emissions were analyzed by Horiba exhaust gas analyzers in the raw exhaust flow (MEXA 7100), as well as in the collection bags (MEXA 7400). The regulated PN emissions were measured following the guidelines of the United Nations Economic Commission for Europe (UNECE) Particle Measurement Programme (PMP). A volatile particle remover (VPR), consisting of an evaporation tube (ET), was used to isolate the solid PN fraction, which was then measured by a condensation particle counter (CPC) manufactured by AVL, with a 50% counting efficiency at 23 nm. The PM was not measured for any of the tests.

Emissions of solid particles smaller than 23 nm are currently unregulated. These were analyzed using a CPC manufactured by TSI (model 3772), with a 50% counting efficiency at 10 nm. This was installed downstream of the VPR. The size distribution of the emitted particles was characterized by an Engine Exhaust Particle Sizer (EEPS) manufactured by TSI (model 3090). The EEPS measured the particle spectrum in 32 discrete bins ranging from 5.6 to 560 nm. For most of the tests, a catalytic stripper (CS) was used upstream of the EEPS to eliminate the volatile fraction. For some tests, the CS was not used upstream of the EEPS. This allowed the examination of the volatile and solid particle spectrums. The particle size spectrum was approximated by a bimodal distribution to estimate and analyze the volatile and solid particle modes.

The measurement of unregulated pollutants in the gaseous phase took place directly in the undiluted tailpipe exhaust flow by high-resolution Fourier-transform infrared spectroscopy (FTIR) with a spectrometer manufactured by AVL, with a 1 Hz temporal resolution. The FTIR measured the concentrations of up to 20 exhaust species; this report discusses only the emissions of ammonia (NH₃), methane (CH₄), nitrous oxide (N₂O), and formaldehyde (HCHO). The data resulting from the FTIR measurements of acetaldehyde and cyanide compounds did not allow a thorough analysis. Thus, these unregulated pollutants are not included in this study.

The location of the different analyzers is shown in Figure 2.

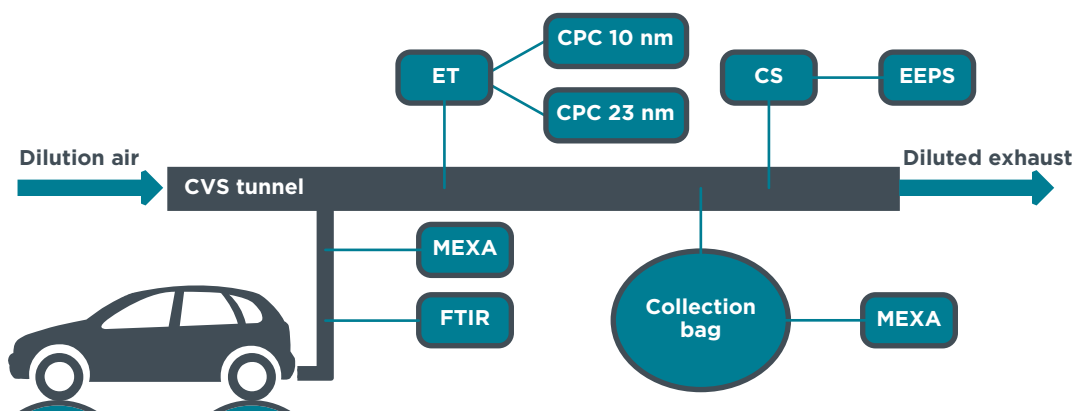


Figure 2. Experimental setup at JRC's VELA facilities
 Notes: FTIR: Fourier transform infrared analyzer. MEXA: Gas analyzer. ET: Evaporation tube. CPC: Condensation particle counter. CS: Catalytic stripper. EEPS: Exhaust particle sizer. CVS: Constant volume sampling.

An on-board data acquisition (DAQ) system recorded additional parameters from the vehicle's information network and directly from the vehicle's sensors, such as the engine speed and torque, air mass flow, and coolant temperature. The DAQ also recorded the signals from additional probes installed in the vehicle. The additional probes, relevant for this study, measured the exhaust temperature upstream and downstream of each TWC, the electric power generation, the engine-out air-fuel ratio, and the tailpipe air-fuel ratio.

TESTS CONDUCTED

The vehicle was tested over the New European Driving Cycle (NEDC), the Worldwide Harmonized Light-duty Test Cycle (WLTC), and two other cycles that mimic the vehicle speed and road-grade profile of a shortened Real-Driving Emissions (RDE) test, one of them with a more challenging urban portion. The speed and grade profiles of these cycles were measured on the road during an RDE test compliant with the regulatory provisions. The chassis dynamometer tests mimic sections of those tests. To avoid confusion, these cycles are referred to as RDC (Real Driving Cycle) and RDC-City, respectively. The speed traces for all cycles, and the road grade for the RDC cycles, are shown in Figure 3.

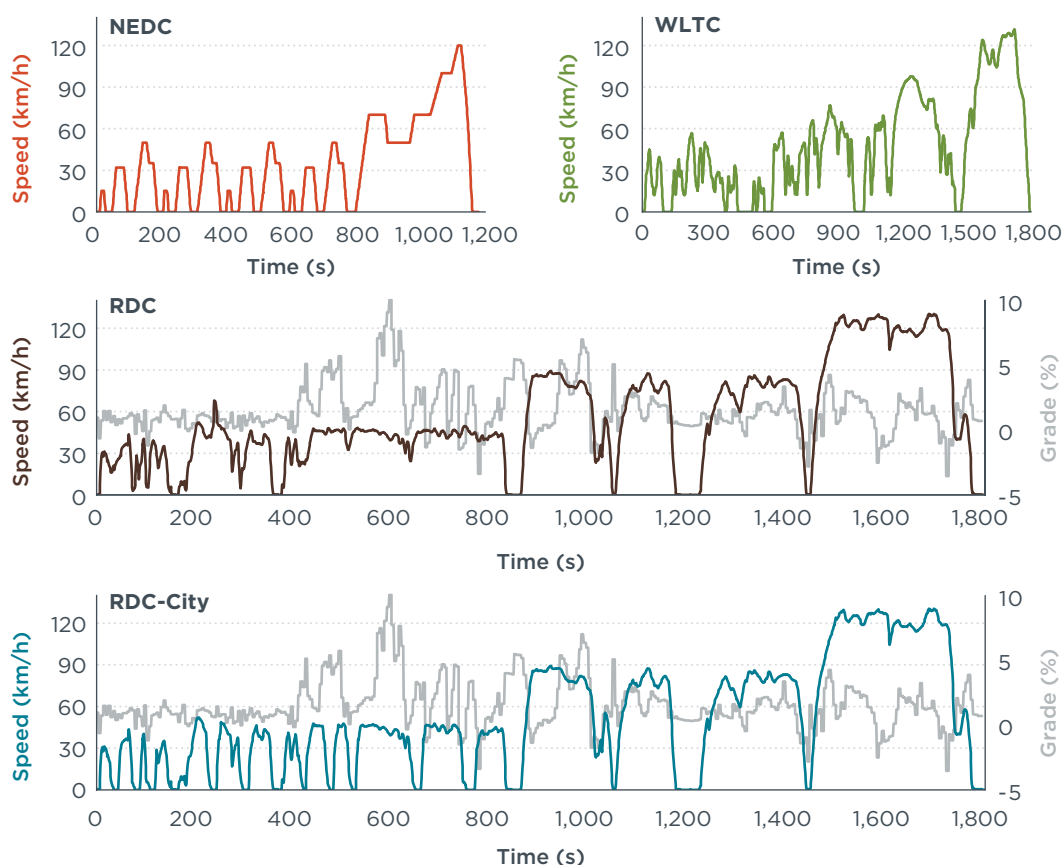


Figure 3. Drive cycles used in chassis dynamometer testing

The tests were performed at different ambient temperatures, ranging from -7°C to 23°C , and starting with cold or hot engine. The standard cold-start tests, with an ambient temperature of 23°C , used for type approval, were performed as required by UNECE Regulation 83 rev05 for the NEDC, and regulation EC 2017/1151 for the WLTC. The vehicle was fueled with commercially available gasoline with a 5% ethanol volume fraction (E5).

The type approval road load parameters were not available, and their determination by coastdown was not part of the scope of the project. Therefore, the road load parameters

applied during the NEDC and WLTC tests where calculated based on the vehicle characteristics, by a methodology already described in the literature (Pavlovic, Marotta, & Ciuffo, 2016; Tsiakmakis, Fontaras, Ciuffo, & Samaras, 2017). The RDC tests used the WLTC road load parameters. For tests at -7°C, the road load parameters were increased by 10%, which is consistent with the Type VI test provisions established in UNECE Regulation 83 rev05.⁷

The test program is summarized in Table 1. Due to the limited availability of some of the instruments, or their malfunction during testing, not all tests resulted in valid measurements. These instances are detailed in the *Results and general discussion* section.

Table 1. Test program

Cycle	Temp.	Start	Runs	Notes
NEDC	23°C	Cold	4	2 runs with no preconditioning
	23°C	Hot	2	
	23°C	Hot	2	Runs with high electric consumer loads ^a
	10°C	Cold	2	
WLTC	23°C	Cold	3	1 run in sports mode
	23°C	Hot	3	1 run in sports mode
	14°C	Cold	2	
RDC	23°C	Cold	2	1 run in sports mode
	23°C	Hot	2	1 run in sports mode
	-7°C	Cold	1	
RDC-City	23°C	Cold	2	1 run in sports mode
	23°C	Hot	2	Runs in sports mode
	-7°C	Cold	1	
	-7°C	Hot	1	

^aDuring these tests, the air conditioning was operated at the lowest temperature and the highest fan speed. Additionally, the vehicles lights were on.

7 To simulate operation at -7°C, UNECE Regulation 83 rev05 (United Nations Economic Commission for Europe, 2015) allows to determine the driving resistance at -7°C (through coastdown) or alternatively to determine road load parameters using the coastdown data at 23°C but reducing the coastdown time by 10%.

RESULTS AND GENERAL DISCUSSION

REGULATED POLLUTANTS

Although the focus of this paper is on unregulated pollutants, Figure 4 summarizes the emissions results of the regulated pollutants. The tabulated results shown in Figure 4 can be found in Table A1 of the Appendix. The emissions over all of the test runs were below the Euro 6 standards, with the exception of the cold-start tests at -7°C. Over these low-temperature tests, the Euro 6 limits were exceeded for nonmethane hydrocarbons (NMHC) and PN (solid, > 23 nm), but not for NO_x and CO. The low temperature PN emissions are up to three times the Euro 6 limit (6×10^{11} #/km) and up to six times the PN emissions measured at 23°C, over the same cycle. These are expected results given that substantial fuel enrichment is required at these low engine temperatures to ensure that enough gasoline evaporates to sustain combustion and to avoid partial or complete misfires. However, this strategy can greatly elevate the emissions of particulates, HC, and CO until the engine warms up. This dependence has been documented in the literature for Euro 6 vehicles (Suarez-Bertoa & Astorga, 2018) and for GDI vehicles outside of the EU market (Badshah, Kittelson, & Northrop, 2016).

Currently, only the emissions of HC and CO are regulated through a low temperature test (type 6 test) over the urban portion of the NEDC test cycle at -7°C. The low temperature limits for CO and HC are 15 and 18 times the Euro 6 limit at 23°C (type 1 test), respectively. These were not exceeded during the -7°C tests.



Figure 4. Tailpipe emission factors over the tested cycles for the regulated pollutants

Notes: The average (bars) and minimum/maximum (error bars) are shown. Only one valid test was run for results without error bar.

ULTRAFINE PARTICULATE EMISSIONS

It has been well established that particulate emissions from mobile sources have direct consequences on the health and well-being of citizens (European Commission & European Environment Agency, 2013). Epidemiological studies show that atmospheric PM is directly linked to premature death and disease in urban populations and that there is no safe threshold below which exposure to ultrafine particles has no effect on mortality and morbidity (World Health Organization, 2016).

The health effects of particulate emissions are caused by the inhalation and penetration of particles into the human body, where both chemical and physical interactions can induce irritation or damage. Depending on the particle size, different deposition mechanisms and deposition locations can be identified (U.S. Environmental Protection Agency [U.S. EPA], 2014b). Figure 5 illustrates the deposition efficiency and the deposition location for particles of different sizes. Coarse particles, generally larger than 2.5 micrometers (μm), readily deposit in the head's nasal, pharyngeal, and laryngeal passages through impaction. Fine particles, between 100 nm and 2.5 μm , have a lower deposition and are primarily deposited by sedimentation in the lung region (bronchioles⁸ and alveoli). Lastly, ultrafine particles, smaller than 100 nm, are deposited by sedimentation and diffusion in the head's and lungs' airways. Ultrafine particles are deemed to be the most damaging as they have high deposition fractions and exhibit a large surface-to-volume ratio. The particle surface area seems to be correlated with the biological activity (Baldauf et al., 2016). Particles can act as Trojan horses, transporting toxic substances adsorbed on their surface into the human body.

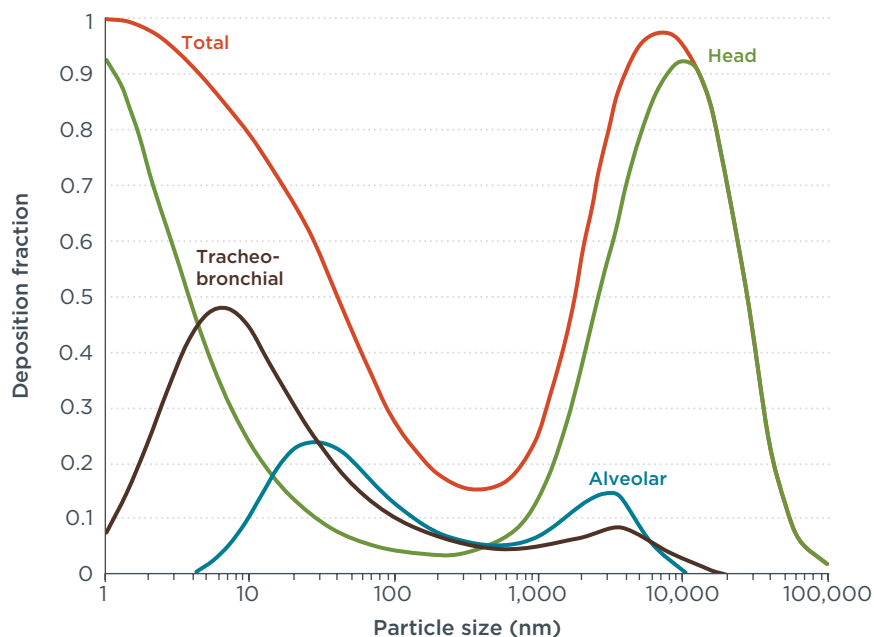


Figure 5. Mathematical model of particle deposition via nasal breathing in the whole lung (total), nose, pharynx and larynx (head), tracheobronchial airways, and alveolar region in healthy adults
Note: Adapted from U.S. EPA (2014b).

The particulate emissions from GDI engines have been the subject of numerous studies over the past decade (Raza, Chen, Leach, & Ding, 2018). The morphology and size distribution of GDI particles is generally different than that of diesel engines (Pfau et al., 2018). Solid particles generated by GDI engines generally have smaller diameters varying from 10 to 100 nm and exhibit a higher fraction of amorphous carbon. In addition to

⁸ The main lung airways are called bronchi. These branch off into smaller passageways, the smallest of which are called bronchioles. At the end of the bronchioles are tiny air sacs called alveoli.

solid particles, GDI engines also emit copious amounts of volatile particles, which can sometimes dominate the PN emissions, and contribute to secondary particle formation (Comte et al., 2017; Platt et al., 2017).

Figure 6 shows a typical particle size distribution for a GDI engine, measured during this study by the EEPS particle size spectrometer, and including both volatile and solid particles. Two clear modes are observable: A nucleation mode smaller than 20 nm, consisting mostly of volatile particles; and an accumulation mode, consisting mostly of solid particles larger than 10 nm. The EEPS classifies particles in 32 discrete bins (green line in Figure 6) based on their electrical mobility.⁹ To convert the electric signals to particle sizes, we used the soot inversion matrix provided by the equipment manufacturer. For the tests done without a VPR upstream of the EEPS, we fit the discrete spectrum to a bimodal distribution (red line in Figure 6) during post-processing. The bimodal distribution consists of two lognormal distributions, one for the nucleation mode (blue line in Figure 6), and one for the accumulation mode (gray line in Figure 6).

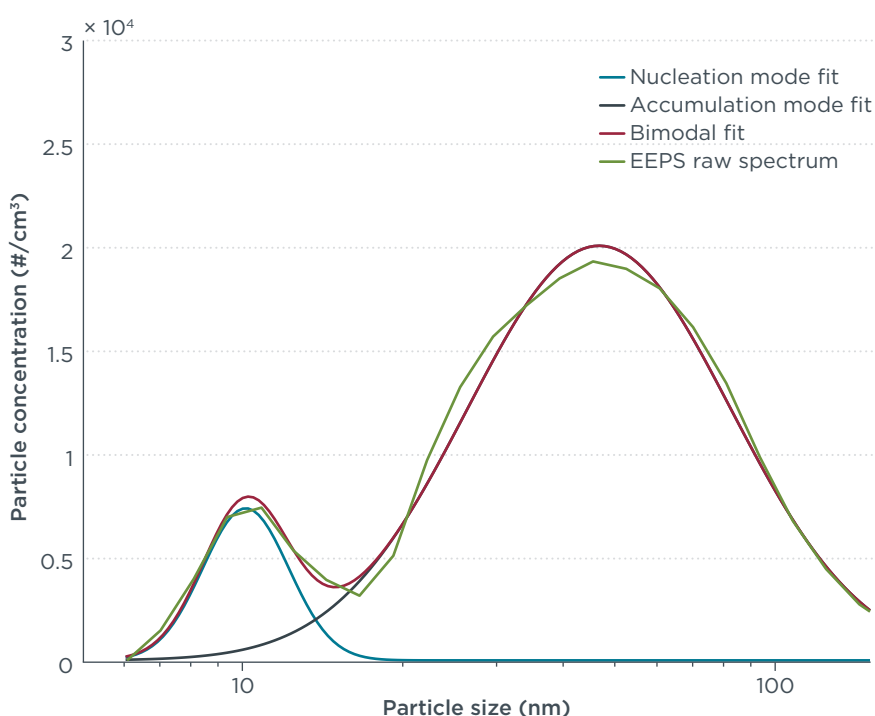


Figure 6. Representative particle distribution measured during this study by the EEPS particle sizer in the diluted flow of the CVS tunnel

Note: The respective lognormal distribution fits for the nucleation and accumulation modes are also shown.

The current regulatory method for determining PN, based on the work of the UNECE's PMP, establishes that the measurements are to be conducted in the diluted exhaust (i.e., in the CVS tunnel). The diluted exhaust gas is passed through a VPR to eliminate the non-solid particles from the sample. A CPC, with 50% detection efficiency at 23 nm, then counts the particles. The size threshold was set at 23 nm because of the repeatability and reproducibility requirements of legislative procedures. Volatile particles are excluded for the same reason. However, the substantial presence of sub-23 nm particles, both volatile and solid, is undisputed.

⁹ Electrical mobility is the ability of charged particles to move through a medium, in this case air, in response to an electric field that is pulling them.

The European Commission has recently funded three projects¹⁰ to develop instruments and methods for the measurement of sub-23 nm solid particles. Similarly, there are ongoing efforts within the UNECE’s PMP group to assess the feasibility of lowering the solid particle size threshold to 10 nm (Giechaskiel et al., 2018).

To be in line with the recent technological and regulatory efforts, targeted at sub-23 nm particles, this analysis focuses mostly on the solid particle emissions. However, the impact of the volatile particles on the total particle count is also addressed at the end of this section.

Solid PN emissions above 10 nm and above 23 nm were measured by two separate CPCs with different cut-off diameters installed downstream of a VPR, as presented in the *Methodology* section. The EEPS particle size spectrometer was used to explore in more detail the particle size distribution in specific events, but not to quantify the total PN emissions.

The distance-specific solid PN emissions over the NEDC and WLTC cycles are summarized in Figure 7. The tabulated results can be found in Table A2 of the Appendix. The results shown correspond to those where the CPC with 10 nm cutoff size functioned properly. The equipment was not available during the RDC and RDC-City chassis dyno tests.

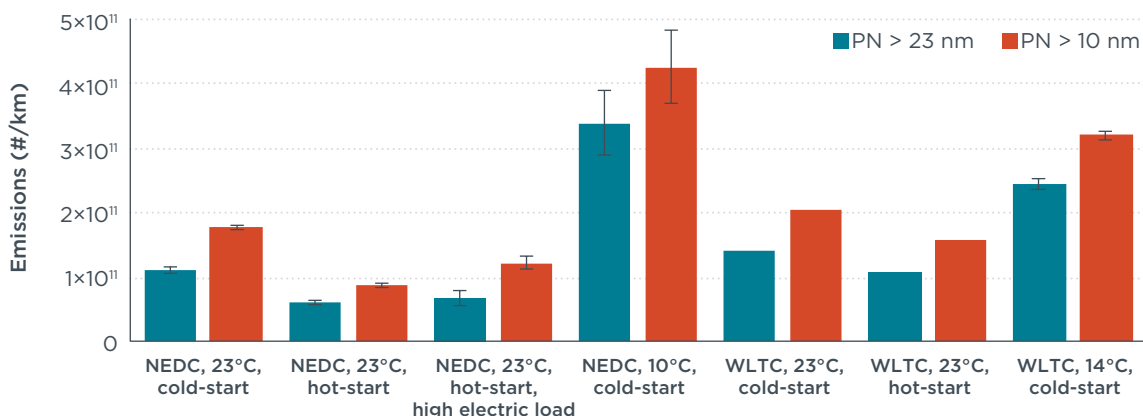


Figure 7. Particulate number per km over the NEDC and WLTC with 23 nm and 10 nm counting thresholds
 Notes: The average and maximum error are shown. Only one valid test was run for results without error bar.

The results in Figure 7 have been corrected to account for particle losses occurring in the VPR. As part of the PMP requirements, the VPR losses of solid particles above 23 nm are quantified and corrected by the particle number concentration reduction factor (PCRF). The PCRF is the average of the particle losses observed at 30 nm, 50 nm and 100 nm. The manufacturer’s calibration was used for measuring solid PN above 23 nm. Because particle losses increase with decreasing particle size, the same calibration is not suitable to correct for the particle losses between 10 nm and 23 nm. Therefore, the particle loss correction in that range was done using the particle losses at 15 nm, and following a methodology previously described in the literature (Giechaskiel, Lähde, & Drossinos, 2019; Giechaskiel et al., 2018). Catalytic strippers are recommended as VPR when measuring sub-23 nm particles, as they reduce the occurrence of measurement artifacts (Giechaskiel, Maricq, et al., 2014). Because a PMP compliant system was used (i.e., one using an evaporation tube as VPR), a re-nucleation artifact downstream from the VPR impacting the sub-23 nm results cannot be ruled out.

¹⁰ The projects funded under the Horizon 2020 program for research and technological development are: DownToTen, Soreal-23, and PEMs4Nano.

Particle losses also take place in the transfer line from the vehicle to the CVS tunnel through agglomeration, thermophoresis, and diffusion. These losses were not quantified, and therefore could not be accounted for. Nevertheless, theoretical estimates show that these losses might reduce tailpipe particle concentrations by up to 17% (Giechaskiel et al., 2019).

The solid PN emissions of the vehicle, above 23 nm, were below the regulatory limit of 6×10^{11} particles/km for all cold and hot-start NEDC and WLTC tests, even though the vehicle did not feature a GPF. The vehicle's solid PN emissions above 10 nm are notably higher than those above the regulatory threshold of 23 nm. However, the inclusion of particles below 23 nm does not increase the solid PN emissions above the regulatory limit. As shown in Figure 8, the fraction of solid particles between 10 nm and 23 nm range from 25% to 114% of the currently regulated PN emissions, with an average value of 50% over all the tests with valid results. The observed 10–23 nm solid particle fractions are consistent with what has been reported for GDI vehicles without a particulate filter (see Table A6 in the Appendix).

The results from this study also suggest that the 10–23 nm PN fraction is inversely proportional to the currently regulated PN emissions (see Figure 8). The PN measurements over the WLTC, particularly over the cold-start tests, show the highest PN emissions but the lowest 10–23 nm fraction, averaging 40%. Conversely, the PN emissions over the NEDC were lower, yet they exhibited a higher 10–23 nm fraction at 65% on average. This trend can also be observed in results published in the scientific literature (Giechaskiel, Manfredi, & Martini, 2014; Giechaskiel, Vanhanen, Väkevä, & Martini, 2017).

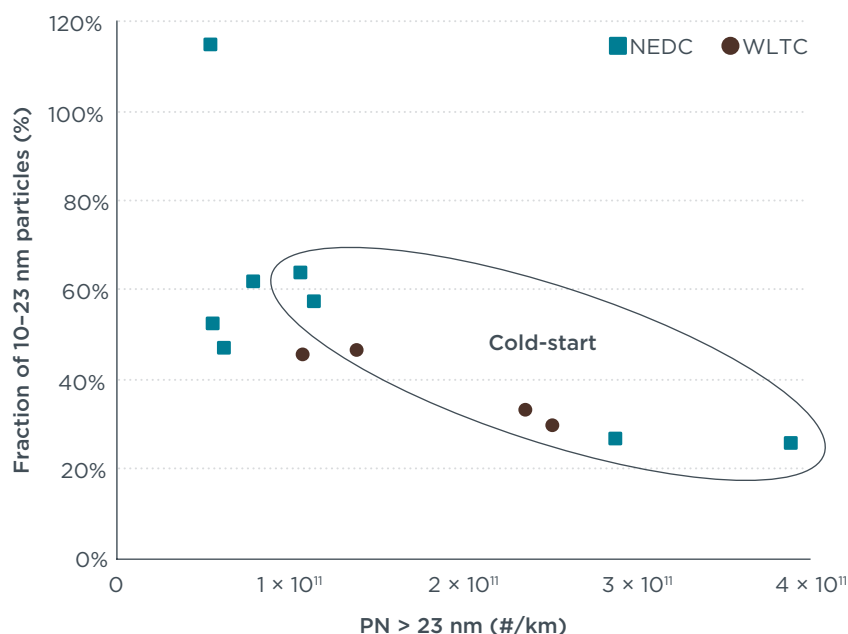


Figure 8. Fraction of solid PN in the 10–23 nm range as measured by condensation particle counters over the tested cycles

A deeper analysis of the PN emissions trace over the drive cycles provides further insight on the sub-23 nm particle fraction. Figure 9 shows the PN (>10 nm and >23 nm) emissions over the cold-start WLTC test at 14°C as an example. The first 20 seconds of operation, encompassing the engine crank-start and first vehicle acceleration, constitute the highest emission period over the complete cycle. Cold crank-start can account for more than 25% of the particulate emissions of the complete cycle (Khalek, 2019);

Rodríguez, 2016). Cold-start particles mostly form when liquid fuel accumulates over the cold surfaces of the combustion chamber and burns during combustion in the absence of sufficient oxygen, leading to the formation of relatively large particles, as shown in the top left of Figure 9. As a result, the 10–23 nm solid particle fraction in the early cold-start phase is lower compared with the rest of the test cycle.

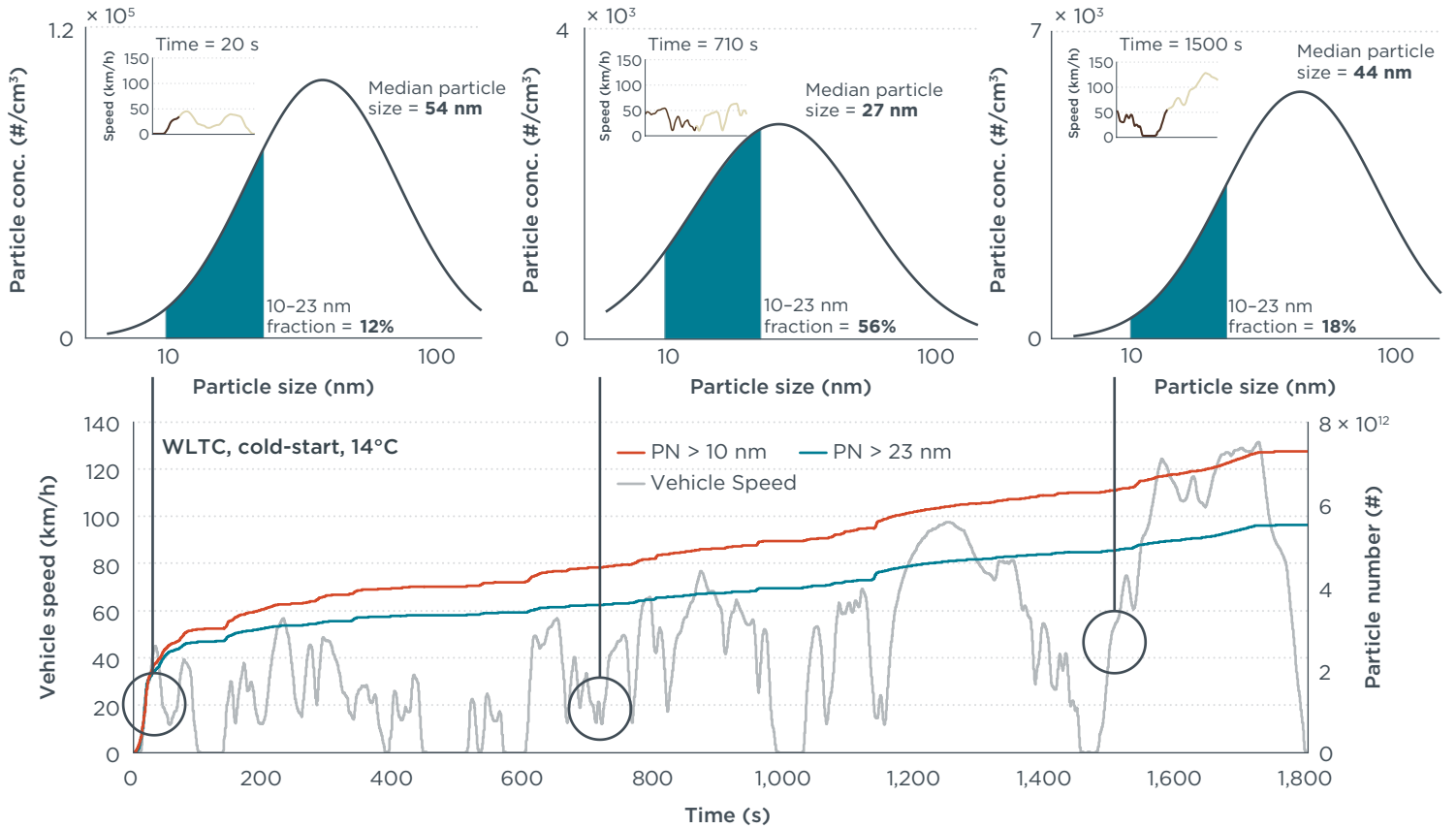


Figure 9. PN emissions over the cold-start WLTC cycle at 14°C ambient temperature
 Notes: The solid PN emissions above 10 nm (red line) and 23 nm (blue line) were measured with CPCs. The size distributions on the top were measured by the EEPS particle sizer in the diluted CVS tunnel, without the use of a VPR.

In warmed-up operation at low and medium loads, characteristic of urban and rural driving (see Figure 9, top center), the median particle size is smaller than in the cold-start and highway periods, as the particle distribution shifts to smaller particle sizes. Thus, the 10–23 nm solid particle fraction is significantly higher. Lastly, during high-load operation, such as in the transition from rural to highway driving, or in sustained high-speed driving (Figure 9, top right), the PN emissions increase once again with a noticeable shift of the particle size distribution to larger sizes. Consequently, the contribution of particles between 10 and 23 nm decreases, compared with low- and medium-load operation.

The EEPS particle size spectrometer was also used to examine the fraction of non-regulated volatile particles (estimated by the nucleation mode fit) in the vehicle’s exhaust. For the test performed without a VPR upstream of the EEPS, the instrument was capable of measuring the complete particle size spectrum, volatiles and solids, above 5.6 nm. Using the lognormal distributions determined during data post-processing (see Figure 6), we calculated the ratio of total PN (i.e., sum of nucleation and accumulation modes) to solid PN (estimated by the accumulation mode fit). The results are shown in Figure 10. Compared with the solid particle fraction only, accounting for volatile particles would increase the particle count between 52% and 78%, depending on the test.

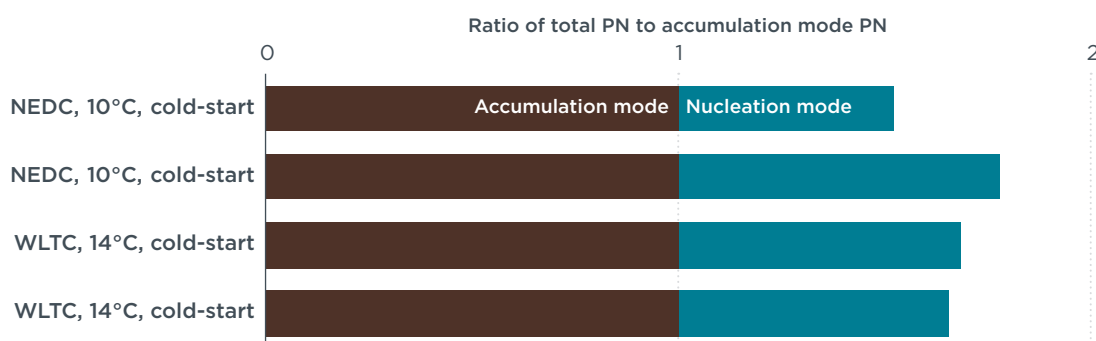


Figure 10. Ratio of total (nucleation and accumulation modes) to solid (accumulation mode) particles over the NEDC tests at 10°C and the WLTC test at 14°C, for which a VPR was not used

The volatile particle fraction range found in this study is within the ranges reported in the literature (see Table A6 in the Appendix). Nevertheless, the formation or evaporation of volatile particles during sampling cannot be ruled out. During mixing in the dilution tunnel, and depending on the dilution conditions, gaseous species in the exhaust gas can nucleate, and volatile particles can evaporate. These particles are known as nucleation and evaporation artifacts. Because the EEPs sampled from the CVS and not directly at the tailpipe, the measured nucleation mode could have been affected by the temperature, pressure, and dilution ratio of the CVS.

Interim conclusion

The findings of this study are consistent with other studies: The sub-23 nm solid PN fraction of GDI engines is significant. Systematic efforts in the context of UNECE's PMP show that the measurement of solid PN emissions down to 10 nm is feasible for legislative purposes. Furthermore, lowering the detection size threshold from the current 23 nm to 10 nm can be achieved without large investments or significant modifications to the existing PMP measurement systems with a 23-nm cutoff (Giechaskiel et al., 2018). However, further effort needs to be placed on characterizing the sub-23 nm particle losses, and on investigating the efficacy and variance of the different instruments and methods, with an emphasis on enabling tailpipe measurements.

Future emissions regulations should consider lowering the PN counting threshold to reflect the current technical feasibility and the epidemiological evidence regarding the higher deposition efficiency of sub-23 nm particles. Furthermore, future regulatory effort should strive for the development of a robust measurement procedure for volatile particles and consider their inclusion in regulatory limits.

AMMONIA

Vehicular ammonia (NH₃) emissions are currently unregulated in the light-duty standards. Heavy-duty engines, on the other hand, are subject to a limit of 10 ppm, averaged over the certification cycle. NH₃ emissions can represent a serious threat to urban air quality, given ammonia's significant role in the formation of secondary particles (Erisman & Schaap, 2004). Although agricultural activity is the main overall source of NH₃ emissions (Backes, Aulinger, Bieser, Matthias, & Quante, 2016), vehicular emissions can surpass the agricultural sector as the main source of NH₃ emissions in urban centers (Fenn et al., 2018; Sun et al., 2017). Urban centers are typically ammonia-limited environments. As a result, NH₃ readily reacts in the atmosphere to form secondary aerosols, such as ammonium nitrate and ammonium sulfate, increasing PM_{2.5} levels (Link et al., 2017; Suarez-Bertoa et al., 2017).

With the reduction in gasoline NO_x emissions achieved in the past decade through the full deployment of TWCs in gasoline engines (Bernard et al., 2018), several studies indicate that NH₃ is becoming the dominant fixed nitrogen compound emitted by stoichiometric spark-ignited engines (Bishop & Stedman, 2015; Link et al., 2017; Suarez-Bertoa & Astorga, 2016a; Suarez-Bertoa & Astorga, 2016b; Suarez-Bertoa et al., 2017). Ammonia is not a byproduct of the combustion process; however, it can be formed in substantial quantities in the TWC through various reaction pathways involving the water-gas-shift reaction of CO and hydrogen (H₂), the steam-reforming of unburned HC, and the reduction of nitric oxide (NO) (Suarez-Bertoa et al., 2015). The ideal conditions for NH₃ production are fuel-rich events with high engine-out CO, H₂, and HC emissions, low oxygen content, and high exhaust temperatures (Bielaczyc, Szczotka, Swiatek, & Woodburn, 2013). These are the conditions encountered during periods of aggressive acceleration or high sustained engine load.

Figure 11 summarizes the measured emissions of NH₃ over the different test cycles. The results are presented as emission factors in units of mg/km, as well as the average NH₃ concentration over the test cycle, to allow a direct comparison with the heavy-duty limit of 10 ppm. The tabulated results can be found in Table A3 of the Appendix. NH₃ emissions ranged from 2.7 mg/km for the cold-start WLTC test at 14°C to 11.2 mg/km for the cold-start RDC-City test at -7°C. The results are consistent with the ranges reported in the scientific literature (see Table A6).

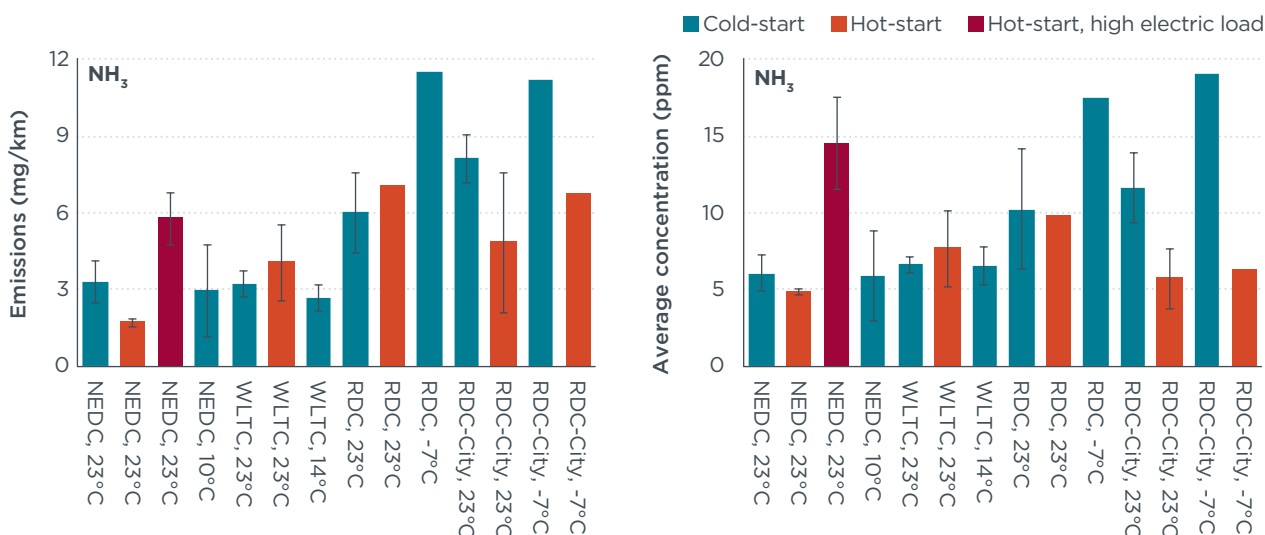


Figure 11. NH₃ emissions and average NH₃ concentration over the tested cycles
 Notes: The average and maximum error are shown. Only one valid test was run for results without error bar.

Compared with the other fixed nitrogen species in the exhaust, NH₃ emissions are approximately half of the NO_x emissions on a mass basis, and are 10% higher than NO_x emissions on a molar basis. NO_x and NH₃ participate in the formation of PM2.5 through the nitrate (NO₃⁻) and ammonium (NH₄⁺) ions. Although the formation of PM2.5 from NO_x and NH₃ is a complex process in atmospheric chemistry, the molar comparison gives a better indication of the relative contribution of each species in secondary particle formation.

The coolant temperature at the start of the test did not have a large impact on the NH₃ emissions over the NEDC and WLTC tests, although significant increases were seen on the RDC at -7°C. Hot-start tests result in higher NH₃ emissions than the cold-start counterparts for the WLTC and RDC tests, but the trend is reversed on the NEDC and RDC-City tests.

Figure 12 shows the NH₃ emission traces for selected cycles, which are representative of the results summarized in Figure 11. In most cases, the stepwise increases in NH₃ emissions occur immediately after periods of heavy acceleration, late in the drive cycle (e.g., in the start of the highway phase). Consistently, three factors drive this phenomenon: high catalyst temperatures, low air/fuel ratios (i.e., fuel enrichment), and high exhaust mass flow. These parameters are all highly dependent on engine calibration.

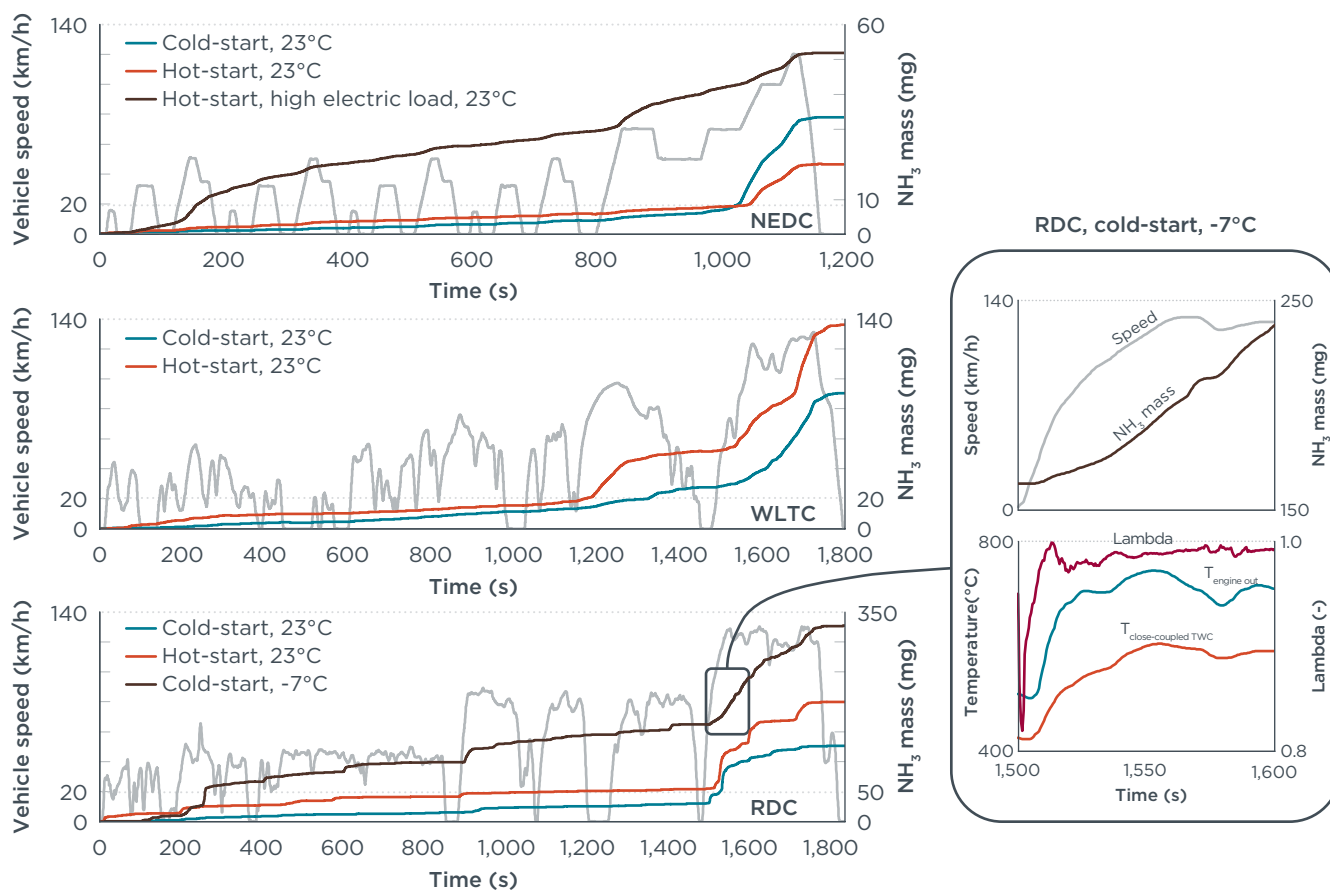


Figure 12. NH₃ emissions over selected test cycles

Using the RDC cold-start test at -7°C as an example, a significant amount of NH₃ is produced in the period from 1,500 to 1,600 seconds (Figure 12, bottom). During this period, and despite the low ambient temperature, the upstream temperature of the close-coupled TWC averages 550°C, the average air/fuel ratio is 2% richer than stoichiometric (i.e., average lambda = 0.98), and the air mass flow averages 110 kg/h. In comparison with the RDC tests at 23°C, the lower ambient temperature triggered a calibration with a slightly richer air-fuel mixture to ensure combustion stability and rapidly warm-up the TWC. As a result, the average lambda over the complete cold-start RDC test at -7°C was 2.6% lower (i.e., richer) than for the tests at 23°C. Despite the lower ambient temperature, the average temperature upstream of the close-coupled TWC was 6.7% higher in the -7°C test than in the 23°C tests.

The results also indicate a high sensitivity of NH₃ emissions to the auxiliary loads on the engine (see Figure 11). Emissions over the hot-start NEDC test at 23°C with a higher load from electric consumers (i.e., air conditioning and lighting systems) are approximately 3 times the emissions over the same cycle without the additional auxiliary loads (Figure 12, top). In the hot-start tests with high electric load, the vehicle uses a richer air-fuel mixture. The average lambda over the tests with high electric load was 5.2% lower (i.e., richer) than for the tests with normal electric load. Furthermore, in the tests with higher

load, the average temperature upstream of the close-coupled TWC was 14% higher than in the test without the additional electric consumption.

In case of rich operation, engine-out CO emissions are directly proportional to the level of enrichment. Given the connection between air-fuel ratio and NH₃ production, it has been proposed that CO emissions from gasoline vehicles are indicative of NH₃ formation over the TWC (Kean et al., 2009; Livingston, Rieger, & Winer, 2009; Suarez-Bertoa, Zardini, & Astorga, 2014). This link was explored in the experimental results from the present study and is shown in Figure 13.

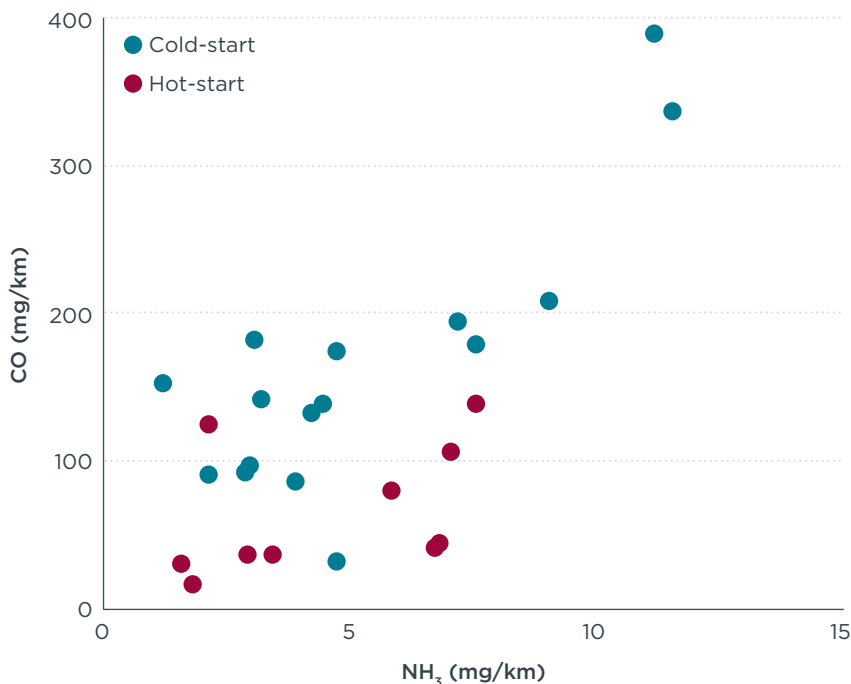


Figure 13. NH₃ and CO emissions scatter plot for all tests, showing no correlation was identified

Figure 13 differentiates between cold-start and hot-start tests. In cold-start tests, CO increases rapidly at the beginning of the cycle, due to the low activity of the TWC, but NH₃ is not produced as catalyst temperatures are low. Hot-start tests remove the differential impact of the cold-start on CO and NH₃, as CO is expected to be formed only in rich operating phases at high loads, which could favor NH₃ formation. However, no strong correlation could be identified for either test group.

Previous studies (Bishop & Stedman, 2015; Bishop, Stedman, Burgard, & Atkinson, 2016) indicate that TWCs increase their NH₃ production as they age. As the aging continues and the catalysts begin to lose their catalytic activity, NH₃ production declines again. Therefore, the NH₃ emission trends reported in this study, and their link to CO emissions, do not necessarily reflect the behavior of vehicles with higher odometer readings.

Interim conclusion

Ammonia emissions have become a significant source of fixed nitrogen species of gasoline exhaust, contributing directly to the formation of secondary particles through atmospheric processes. The results contribute to the wealth of evidence highlighting the need to regulate vehicular NH₃ emissions. The results from this study, summarized in Figure 14, suggest that a correlation exists between the average NH₃ concentration and the distance-specific NH₃ emissions over the regulatory chassis dynamometer cycles (i.e., cold-start NEDC and WLTC). However, if NH₃ emissions are to be regulated as part of the RDE procedures, a distance-specific NH₃ limit (in mg/km) would provide a more robust approach, in comparison with limiting the average NH₃ concentration as is currently done for heavy-duty engines.

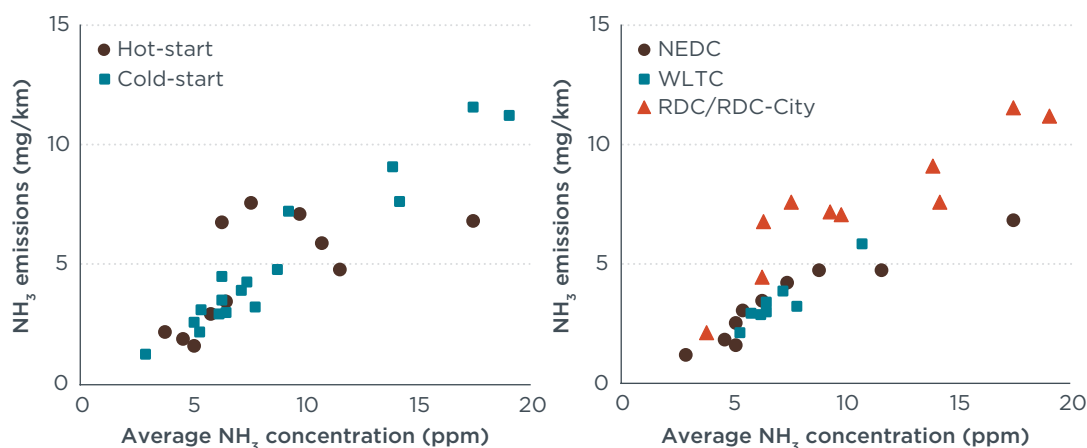


Figure 14. Correlation between average NH₃ concentration and distance-specific NH₃ emissions, clustered by hot-start vs. cold-start and by test type

GREENHOUSE GASES

Methane (CH₄) and nitrous oxide (N₂O) are both powerful greenhouse gases (GHGs) that can be found in significant quantities in the exhaust of motor vehicles. The 20-year global warming potentials (GWPs)¹¹ of these two species are 84 and 264 respectively (Intergovernmental Panel on Climate Change [IPCC], 2013). Due to the short atmospheric lifetime of CH₄ (~12 years), but the long atmospheric lifetime of N₂O (~120 years), the 100-year GWP of CH₄ decreases to 28, but the GWP for N₂O is slightly higher at 265 (IPCC, 2013).

CH₄ emissions occur as a result of incomplete combustion. During combustion, gasoline is broken up into consecutively smaller hydrocarbons until it is fully converted into water and CO₂ in the case of complete combustion. CH₄ is a major intermediate product in these reaction processes (Kar & Cheng, 2009). If there is not a high enough temperature or enough time to complete the combustion reaction, CH₄ escapes the engine in the exhaust gases. Methane is the least reactive hydrocarbon, and high energy is required to break the primary carbon-hydrogen bond. In practical terms, this means that higher temperatures are required for the TWC to achieve high CH₄ conversion rates, when compared with other longer-chained hydrocarbons (Raj, 2016).

CH₄ emissions are implicitly regulated in current emissions legislation in the European Union, as total HC emissions are limited to 100 mg/km under the legislation on vehicles with positive ignition. However, this limit is not driven by the climate-forcing impacts of CH₄ but rather by the need to limit the emissions of other more reactive and toxic hydrocarbons. In the United States, a CH₄ limit has existed for light-duty vehicles since 2012. The applicable limit is 18.8 mg/km over the Federal Test Procedure (FTP) test.

N₂O does not form as a byproduct of combustion but is formed inside the TWC. During the catalytic reduction of NO_x to nitrogen, N₂O forms as an intermediate product. At high enough temperatures, the TWC is effective in reducing NO directly to nitrogen. However, at lower temperatures, an alternative reaction pathway takes place, forming N₂O as an intermediate product (Behrentz, Ling, Rieger, & Winer, 2004). The ideal conditions for the net production of N₂O are when the TWC has warmed sufficiently to show some catalytic activity, but has not yet reached full operating temperature (Graham, Belisle, & Rieger, 2009).

¹¹ The GWP is a measure of how much heat a gas traps in the atmosphere up to a specific time horizon, relative to CO₂.

It has also been reported that the composition of the TWC (i.e., loading of precious metals) has a significant effect on N₂O production. Rhodium, platinum, and palladium differ significantly in their propensity to produce N₂O. Rhodium produces the largest rates of N₂O at low temperatures, but quickly falls at higher temperatures. Palladium gives rise to N₂O at the lowest temperature and also gives the highest concentrations at temperatures above 350°C. Platinum produces the least N₂O (Cant, Angove, & Chambers, 1998).

N₂O emissions are not regulated in the current emissions legislation in the European Union. In the United States, an N₂O limit has existed for light-duty vehicles since 2012; the applicable limit is 6.3 mg/km over the FTP cycle. Chinese emission standards, China 6, limit N₂O emissions to 20 mg/km.

Figure 15 summarizes the measured distance-specific emissions of CH₄ and N₂O over the different test cycles. The results are presented as emission factors for each species, in units of mg/km, as well as the total CO₂-equivalent emissions (i.e., CH₄ and N₂O combined) in units of g/km. The emissions of CH₄ and N₂O are converted to equivalent grams of CO₂ using the aforementioned 20-year and 100-year GWPs.

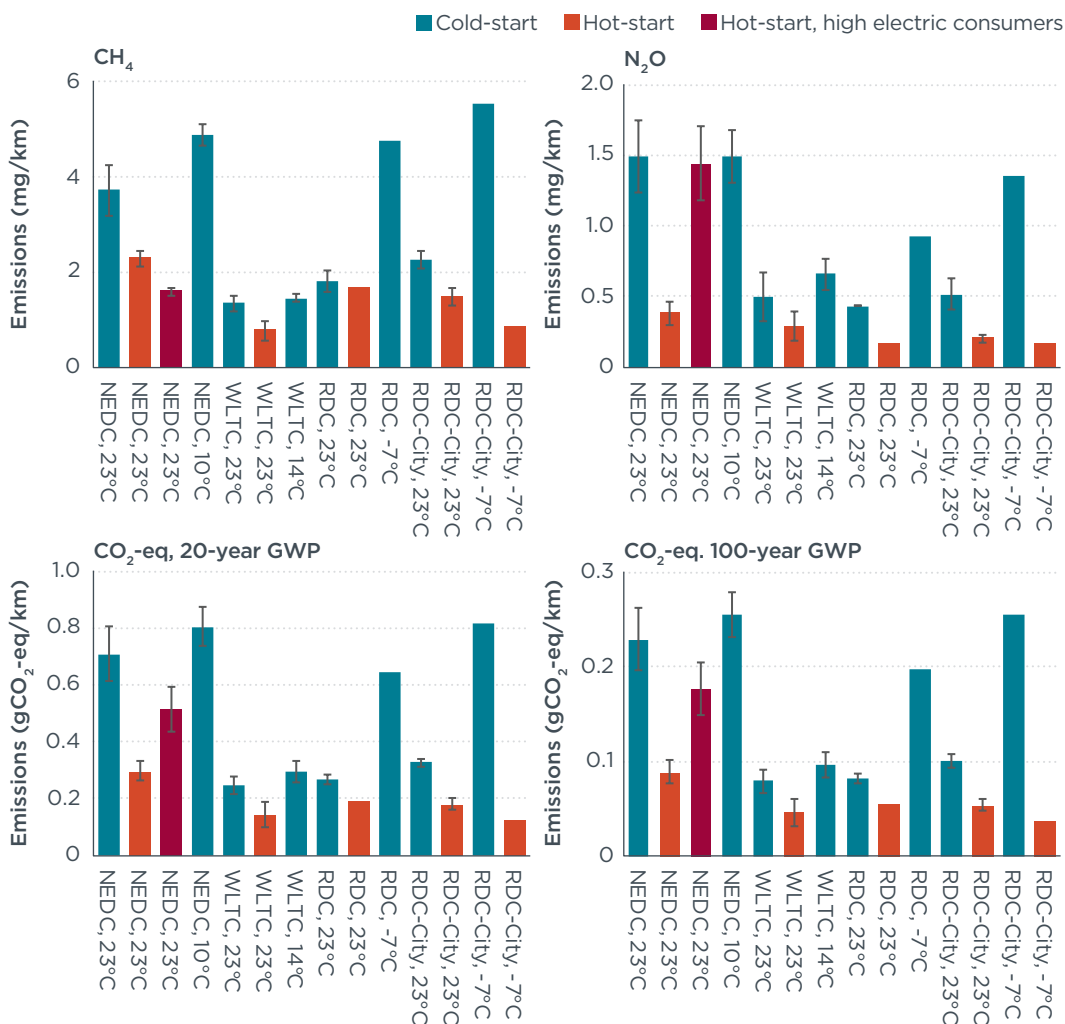


Figure 15. CH₄ and N₂O emission factors, and their combined 20-year and 100-year CO₂ equivalence, over the NEDC, WLTC, RDC, and RDC-City tests
 Notes: The average and maximum error are shown. Only one valid test was run for results without error bar.

N₂O emissions ranged from 0.2 mg/km for the hot-start RDC tests (at both 23°C and -7°C), to 1.5 mg/km for the cold-start NEDC tests (at both 23°C and 10°C). CH₄ emissions ranged from 0.8 mg/km for the hot-start WLTC test at 23°C to 4.9 mg/km for the cold-start NEDC test at 10°C. The N₂O results are consistent, although in the lower end,

with the values reported in the scientific literature for gasoline vehicles equipped with TWC and fueled with low sulfur gasoline (see Table A6). CH₄ emissions are in the range reported in the literature (see Table A6).

In general, CH₄ and N₂O emissions in stoichiometric gasoline engines are predominantly an issue of insufficient catalytic activity at the beginning of the driving cycle. To illustrate this fact, Figure 16 shows the cumulative CH₄ and N₂O emissions over the cold- and hot-start WLTC at 23°C. The first 50 seconds of the cold-start test are responsible for 56% of CH₄ emissions and 72% of N₂O emissions. During the hot-start test, the first 50 seconds account for 25% and 65% of the CH₄ and N₂O emissions, respectively.

N₂O and CH₄ emissions are higher over the NEDC than the WLTC because the NEDC is less transient and has more idling time than WLTC. This means the engine and aftertreatment take longer to reach their optimal operation temperature. For the same reason, the emissions over the RDC-City test tend to be higher than those over the RDC test.

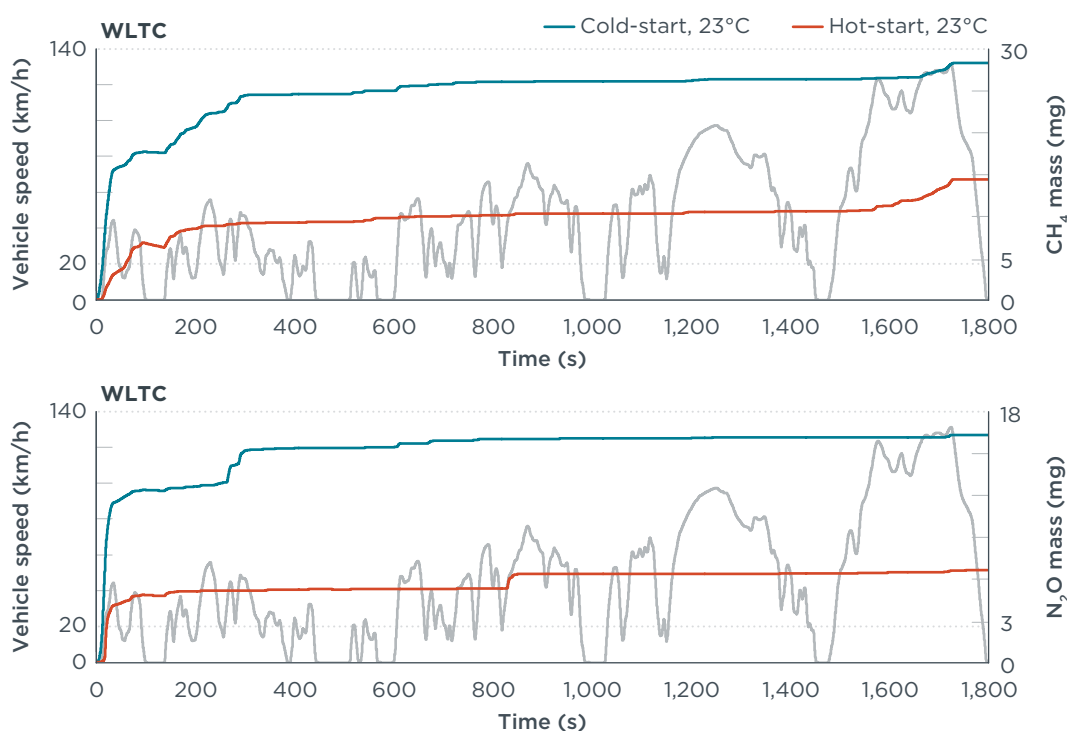


Figure 16. CH₄ and N₂O emissions over the cold-start and hot-start WLTC tests at 23°C ambient temperature

Figure 17 shows the combined emissions from CH₄ and N₂O, in equivalent grams of CO₂, as a percentage of the CO₂ emissions over all the tests performed in this study. Using the 20-year GWPs, the combined emissions of CH₄ and N₂O account for up to 0.75% of the vehicle's GHG footprint. That figure drops to 0.25% when using the 100-year GWPs. Previous studies (Nevalainen et al., 2018; Winer & Behrentz, 2005) suggest that the N₂O production increases with TWC aging. Therefore, the N₂O emission trends reported in this study do not necessarily reflect the behavior of vehicles with higher odometer readings.

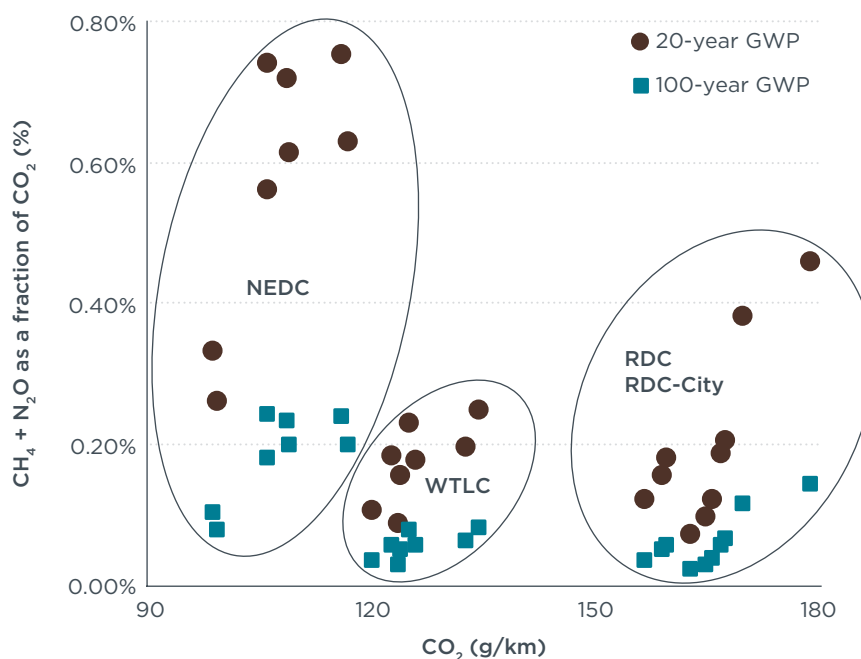


Figure 17. Combined CO₂-equivalent emissions of CH₄ and N₂O, adjusted by their 20- and 100-year GWPs, as a percentage of the measured CO₂ emissions over the different cycles

Interim conclusion

CH₄ and N₂O emissions can both be found in non-negligible amounts in the exhaust gas of the tested Euro 6 gasoline vehicle. Since both species are strong GHGs, their contribution to the climate impact of gasoline vehicles should receive a closer examination. In particular, N₂O emissions are highly dependent on the TWC formulation and on the warm-up strategy of the aftertreatment system. Given the strong climate-forcing effect of CH₄ and N₂O, their emissions should be properly accounted for in the fleet-averaged CO₂ emissions of a manufacturer. The United States Environmental Protection Agency (U.S. EPA) established limits for light-duty emissions of N₂O and CH₄, applicable for vehicles with model year 2012 onward. The applicable limit in the United States is 0.01 g/mile for N₂O and 0.03 g/mile for CH₄ over the FTP cycle. It is recommended for the European Union to include these pollutants in its regulatory framework as well.

ALDEHYDES

Aldehydes are a group of organic compounds containing the functional group -CHO. Aldehydes in the atmosphere are primarily a result of direct emissions from industrial and mobile sources, and secondarily from photochemical reactions (Altemose et al., 2015). The two most common aldehydes emitted from mobile sources are formaldehyde (HCHO) and acetaldehyde (MeCHO), mainly from vehicles fuel with gasoline-ethanol blends (Manzetti & Andersen, 2015).

Exposure to aldehydes presents a significant health risk, yet the mechanisms of aldehyde toxicity are poorly understood. Nevertheless, the genotoxicity of HCHO and MeCHO has been established; both aldehydes can cause nasopharyngeal cancer in humans and have been shown to instigate respiratory carcinomas in rodent models (LoPachin & Gavin, 2014). U.S. EPA classifies both aldehydes as probable human carcinogens (Walsh, 2003), and has set an HCHO limit of 4 mg/mi for the U.S. Tier 3 standards (U.S. EPA, 2014a).

Emissions of HCHO and MeCHO from spark-ignited engines are predominantly the result of partial oxidation of the alcohol and gasoline content of the fuel. Aldehydes are

mainly emitted during the cold-start phase. Although HCHO is present in the exhaust gas of engines fueled with pure gasoline (E0), its presence steadily increases with the fuel's ethanol fraction. On the other hand, MeCHO is primarily produced from the partial oxidation of ethanol, and its presence is negligible when the engine is fueled with E0. However, as the ethanol fraction increases above 10%, MeCHO rapidly overtakes HCHO as the dominant aldehyde (Jin et al., 2017).

Figure 18 summarizes the distance-specific emissions of HCHO over the test cycles measured in this study. Although the emissions of MeCHO were also measured by the FTIR, the results are not presented due to the high test-to-test variability observed, the uncertain background concentration, device calibration, and high signal noise.

HCHO emissions ranged from 0 mg/km (i.e., below the detection limit for the instrument) for all hot-start RDC tests, to 0.23 mg/km for the cold-start NEDC tests. As expected, HCHO emissions over the NEDC and WLTC are several times higher in the cold-start tests than in the hot-start ones. The HCHO results are consistent with the values reported in the scientific literature for gasoline vehicles (see Table A6).

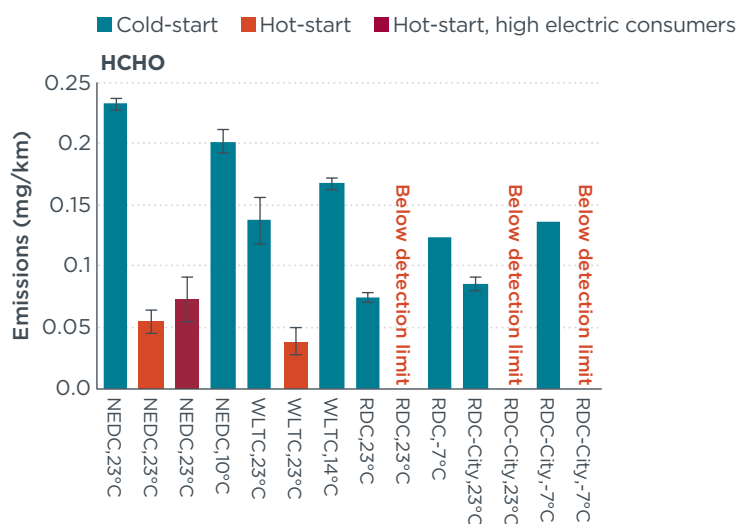


Figure 18. HCHO emissions over the test cycles

Notes: The average and maximum error are shown. Only one valid test was run for results without error bar.

The results from this study corroborate previous findings that HCHO emissions are predominantly a cold-start phenomenon. Figure 19 shows the cumulative HCHO emissions over the cold- and hot-start NEDC and WLTC tests at 23°C, and over the RDC cold-start tests at 23°C and -7°C.

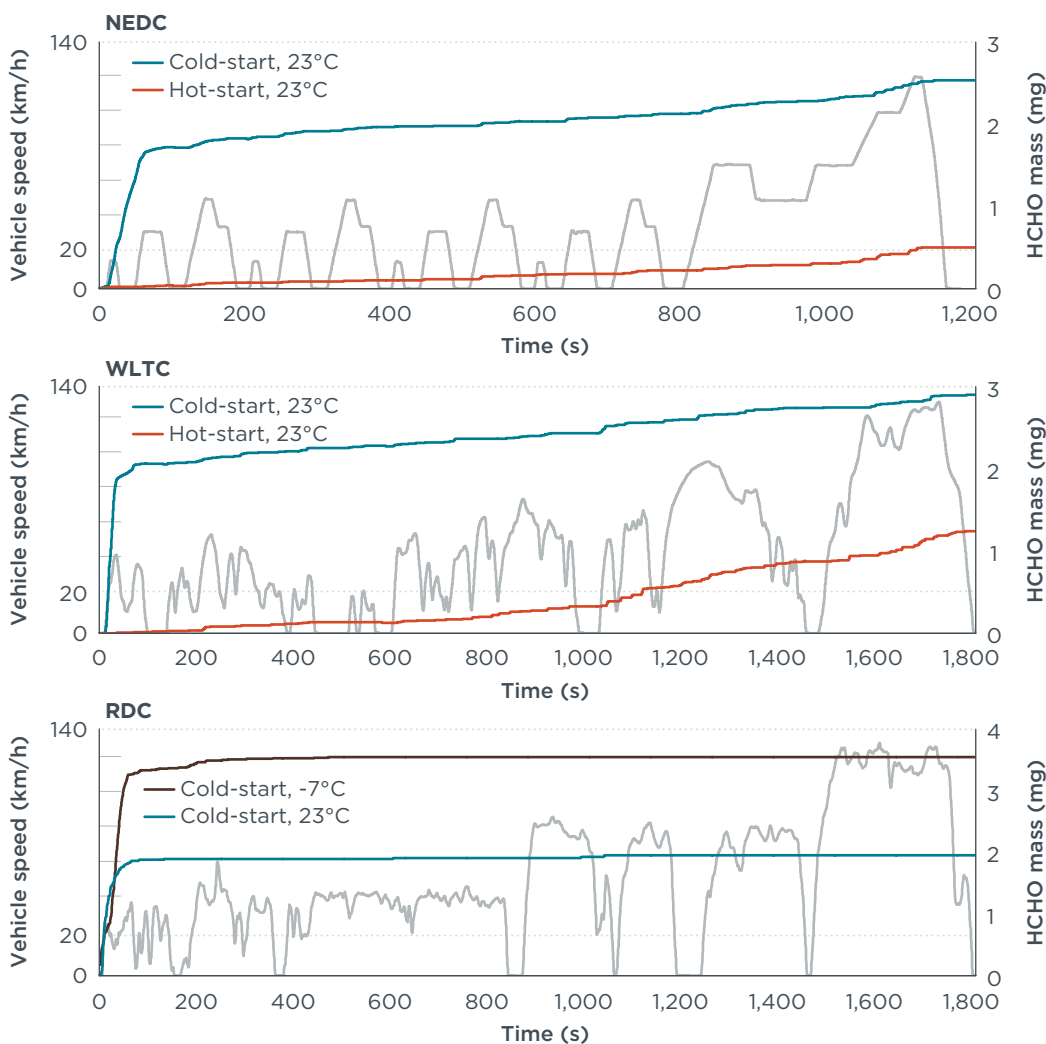


Figure 19. HCHO emissions over selected test cycles

The first minute of operation over the cold-start test is responsible for approximately 70% of the HCHO emissions over the NEDC and WLTC, and for more than 90% over the RDC cycle. This is an expected result given the higher reactivity of HCHO and MeCHO in the TWC, compared with other hydrocarbons such as aromatics and alkanes (Bogarrra et al., 2017). The higher dynamicity of the RDC cycle allows a faster warm-up of the aftertreatment system, constraining the HCHO emissions mostly to the first minute of operation. Comparing the RDC cold-start tests at -7°C and the WLTC cold-start tests at 23°C, the former achieves 350°C at the underfloor TWC after 350 seconds. It took 750 seconds to achieve the same temperature over the WLTC tests.

Interim conclusion

HCHO emissions can be found in non-negligible amounts in the exhaust gas of the tested Euro 6 vehicle fueled with E5. Formaldehyde emissions were constrained to the cold-start test and were mostly emitted in the first minute of operation. Given the high toxicity of HCHO and other aldehydes, this non-regulated pollutant should receive a closer examination, particularly if the market share of flex-fuel vehicles increases or if gasoline-ethanol blends with a higher alcohol fraction are introduced.

SUMMARY AND POLICY RECOMMENDATIONS

In this study, a C-segment passenger vehicle, equipped with a gasoline direct injection engine and compliant with the Euro 6c standard, was tested on the chassis dynamometer over the regulatory NEDC and WLTC cycles, and over two RDE-like cycles. The tests were performed at different ambient conditions and with both cold and warmed-up engines. The analysis focused on the emissions of the following types of pollutants:

1. Regulated pollutants
2. Particulate emissions with a size between 10 and 23 nm
3. Ammonia
4. Methane and nitrous oxide
5. Aldehydes

The vehicle exhibited good emissions performance for regulated pollutants. The emissions over all test runs were below the Euro 6 standards, with the exception of the cold-start tests at -7°C. Over these low-temperature tests, the Euro 6 limits were exceeded for HC and PN, but not for NO_x and CO. The low-temperature PN emissions are up to three times the Euro 6 limit (6×10^{11} #/km) and up to six times the PN emissions measured at 23°C over the same cycle.

The number of particles in the 10–23 nm size is substantial. If these particles had been accounted for in the tested vehicle, the total PN emissions would have been 25% to 114% higher. The results from this study are consistent with the data available in the literature and suggest that the 10–23 nm PN fraction is inversely proportional to the total PN emissions. For a given GDI engine, the median size of the emitted particles and the number of particles emitted are usually tied to each other. High-emission events also shift the particle size distribution to larger diameters. Consequently, as manufacturers strive to reduce the regulated PN emissions of GDI engines, the solid particle fraction in the unregulated 10–23 nm range is expected to become more significant.

Ammonia emissions are a result of the reduction of NO_x in the three-way catalyst in an oxygen-deprived, high-temperature environment. These conditions are encountered in the fuel-rich excursions typical of aggressive transient operation or during sustained high engine load. The widespread introduction of three-way catalysts on stoichiometric gasoline engines in the past two decades led to an effective reduction in NO_x emissions. Ammonia emissions are therefore becoming a significant source of reactive nitrogen compound in gasoline exhaust. The results of the measurements from this study show that ammonia emissions are comparable to the emissions of NO_x. They amounted to half the mass NO_x emissions and were 10% higher than the molar NO_x emissions.

Methane and nitrous oxide are both powerful greenhouse gases. While methane emissions are the result of incomplete combustion and low oxidation rates in the three-way catalyst, nitrous oxide forms in the three-way catalyst as a consequence of low catalytic activity. However, once the three-way catalyst achieves its operating temperature, the tailpipe emissions of methane and nitrous oxide drop significantly. The emissions of these two compounds are highly dependent on the TWC formulation and on the warm-up strategy of the aftertreatment system.

Aldehydes are highly toxic substances that can be found in non-negligible amounts in the exhaust gas of gasoline vehicles, particularly when fueled with gasoline-ethanol blends. Formaldehyde emissions were constrained to the cold-start test and were

mostly emitted in the first minute of operation, due to the low temperature of the aftertreatment system. Formaldehyde emissions are regulated in the United States.

POLICY RECOMMENDATIONS

The discussions on the post-Euro 6 era of emissions regulations have begun. While there are many issues that must be addressed in the ongoing and upcoming discussions, this study highlights the importance of extending the set of regulated pollutants, using the testing results of a gasoline direct injection vehicle as an example. In particular, we offer the following recommendations:

1. **Extend the requirements of the low temperature test (type 6 test) at -7°C to include all regulated pollutants, in particular PN emissions.** Furthermore, the current type 6 test limits for CO and HC, which are set at 15 and 18 times the Euro 6 limit, should be adjusted downward.
2. **Reduce the size threshold for particle counting from 23 nm to 10 nm.** The technical feasibility of measuring sub-23 nm particles has been discussed at length in UNECE's Particle Measurement Programme. The results of this working group suggest that lowering the current detection size threshold from 23 nm down to 10 nm for solid particles is possible without large investment costs or significant modifications to existing measurement systems. The inclusion of volatile particles and the measurement of the PN at the tailpipe should also be considered for the development of future methodologies.
3. **Introduce technology- and application-neutral limits for vehicular ammonia emissions.** Ammonia contributes directly to the formation of secondary particles through atmospheric processes. Although agricultural activity is the main overall source of ammonia, vehicular emissions can surpass the agricultural sector as the main ammonia source in urban centers. A solid methodology already exists to measure ammonia emissions in the laboratory, and pilot tests using portable FTIR systems indicate that ammonia measurements could also be included in future RDE procedures. A distance-specific limit in mg/km is suggested, in combination with a concentration limit, in ppm, to avoid ammonia spikes that can be detected by the human nose at low concentrations and are perceived as unpleasant.
4. **Establish technology- and application-neutral limits for methane and nitrous oxide emissions, or account for their CO₂-equivalent emissions in the CO₂ standards.** Methane and nitrous oxide have a strong global warming potential, the latter having a longer atmospheric lifetime and a higher global warming potential. Nitrous oxide and methane limits already exist in the United States and China, and it is recommended for the European Union to include these pollutants in its regulatory framework as well. Similar to ammonia, a solid methodology already exists to measure methane and nitrous oxide emissions in the laboratory. The future use of portable FTIR systems can provide an avenue to include these pollutants in the RDE framework.
5. **Introduce technology- and application-neutral limits for vehicular formaldehyde emissions.** Formaldehyde is a highly toxic organic compound that can be found in the exhaust of spark-ignited engines, particularly if fueled with ethanol blends. Formaldehyde emissions increase with the ethanol content of the fuel blend. Therefore, it is recommended that a technology- and application-neutral formaldehyde limit is introduced to reduce the risk that an increase in the ethanol concentration in fuel blends, or an uptake in flex-fuel vehicles, results in an increase in the atmospheric concentration of this genotoxic compound.

REFERENCES

- Altemose, B., Gong, J., Zhu, T., Hu, M., Zhang, L., Cheng, H., ... Zhang, J. (2015). Aldehydes in relation to air pollution sources: A case study around the Beijing Olympics. *Atmospheric Environment (Oxford, England: 1994)*, 109, 61-69. <https://doi.org/10.1016/j.atmosenv.2015.02.056>
- Backes, A. M., Aulinger, A., Bieser, J., Matthias, V., & Quante, M. (2016). Ammonia emissions in Europe, part II: How ammonia emission abatement strategies affect secondary aerosols. *Atmospheric Environment*, 126, 153-161. <https://doi.org/10.1016/j.atmosenv.2015.11.039>
- Badshah, H., Kittelson, D., & Northrop, W. (2016). Particle emissions from light-duty vehicles during cold-cold start. *SAE International Journal of Engines*, 9(3), 1775-1785. <https://doi.org/10.4271/2016-01-0997>
- Baldauf, R. W., Devlin, R. B., Gehr, P., Giannelli, R., Hassett-Sipple, B., Jung, H., ... Walker, K. (2016). Ultrafine particle metrics and research considerations: Review of the 2015 UFP Workshop. *International Journal of Environmental Research and Public Health*, 13(11). <https://doi.org/10.3390/ijerph13111054>
- Behrentz, E., Ling, R., Rieger, P., & Winer, A. M. (2004). Measurements of nitrous oxide emissions from light-duty motor vehicles: A pilot study. *Atmospheric Environment*, 38(26), 4291-4303. <https://doi.org/10.1016/j.atmosenv.2004.04.027>
- Bernard, Y., Tietge, U., German, J., & Muncrief, R. (2018). *Determination of real-world emissions from passenger vehicles using remote sensing data*. Retrieved from the International Council on Clean Transportation website: <https://www.theicct.org/publications/real-world-emissions-using-remote-sensing-data>
- Bielaczyc, P., Szczotka, A., Swiatek, A., & Woodburn, J. (2013). Investigations of ammonia emissions from Euro 5 passenger cars over a legislative driving cycle. *Proceedings of the FISITA 2012 World Automotive Congress*, 671-685. Springer Berlin Heidelberg.
- Bishop, G. A., & Stedman, D. H. (2015). Reactive nitrogen species emission trends in three light-/medium-duty United States fleets. *Environmental Science & Technology*, 49(18), 11234-11240. <https://doi.org/10.1021/acs.est.5b02392>
- Bishop, G. A., Stedman, D. H., Burgard, D. A., & Atkinson, O. (2016). High-mileage light-duty fleet vehicle emissions: Their potentially overlooked importance. *Environmental Science & Technology*, 50(10), 5405-5411. <https://doi.org/10.1021/acs.est.6b00717>
- Bogarra, M., Herreros, J. M., Hergueta, C., Tsolakis, A., York, A. P., & Millington, P. J. (2017). Influence of three-way catalyst on gaseous and particulate matter emissions during gasoline direct injection engine cold-start. *Johnson Matthey Technology Review*, 61(4), 329-341.
- Cant, N. W., Angove, D. E., & Chambers, D. C. (1998). Nitrous oxide formation during the reaction of simulated exhaust streams over rhodium, platinum and palladium catalysts. *Applied Catalysis B: Environmental*, 17(1), 63-73. [https://doi.org/10.1016/S0926-3373\(97\)00105-7](https://doi.org/10.1016/S0926-3373(97)00105-7)
- Chan, T. W., Meloche, E., Kubsh, J., Brezny, R., Rosenblatt, D., & Rideout, G. (2013). Impact of ambient temperature on gaseous and particle emissions from a direct injection gasoline vehicle and its implications on particle filtration. *SAE International Journal of Fuels and Lubricants*, 6(2), 350-371. <https://doi.org/10.4271/2013-01-0527>

- Comte, P., Czerwinski, J., Keller, A., Kumar, N., Muñoz, M., Pieber, S., ... Heeb, N. (2017). *GASOMEP: Current status and new concepts of gasoline vehicle emission control for organic, metallic and particulate non-legislative pollutants* (Final scientific report of the CCEM-Mobility project 807). Retrieved from <https://www.empa.ch/documents/56164/1183406/GASOMEP+Final+Scientific+Report+2017+submitted+Nov.pdf>
- Council of the European Union. (1970). Council Directive 70/220/EEC of 20 March 1970 on the approximation of the laws of the Member States relating to measures to be taken against air pollution by gases from positive-ignition engines of motor vehicles. *Official Journal of the European Union*, L 76. Retrieved from <https://eur-lex.europa.eu/eli/dir/1970/220/oj>
- Council of the European Union. (1972). Council Directive 72/306/EEC of 2 August 1972 on the approximation of the laws of the Member States relating to the measures to be taken against the emission of pollutants from diesel engines for use in vehicles. *Official Journal of the European Union*, L 190. Retrieved from <https://eur-lex.europa.eu/eli/dir/1972/306/oj>
- Council of the European Union. (1983). Council Directive 83/351/EEC of 16 June 1983 amending Council Directive 70/220/EEC on the approximation of the laws of the Member States relating to measures to be taken against air pollution by gases from positive- ignition engines of motor vehicles. *Official Journal of the European Union*, L 197. Retrieved from <https://eur-lex.europa.eu/eli/dir/1983/351/oj>
- Council of the European Union. (1988). Council Directive 88/436/EEC of 16 June 1988 amending Directive 70/220/EEC on the approximation of the laws of the Member States relating to measures to be taken against air pollution by gases from engines of motor vehicles (Restriction of particulate pollutant emissions from diesel engines). *Official Journal of the European Union*, L 214. Retrieved from <https://eur-lex.europa.eu/eli/dir/1988/436/oj>
- Council of the European Union. (1991). Council Directive 91/441/EEC of 26 June 1991 amending Directive 70/220/EEC on the approximation of the laws of the Member States relating to measures to be taken against air pollution by emissions from motor vehicles. *Official Journal of the European Union*, L 242. Retrieved from <https://eur-lex.europa.eu/eli/dir/1991/441/oj>
- Erismann, J. W., & Schaap, M. (2004). The need for ammonia abatement with respect to secondary PM reductions in Europe. *Environmental Pollution*, 129(1), 159-163. <https://doi.org/10.1016/j.envpol.2003.08.042>
- European Commission. (1977). Commission Directive 77/102/EEC of 30 November 1976 adapting to technical progress Council Directive 70/220/EEC of 20 March 1970 on the approximation of the laws of the Member States relating to measures to be taken against air pollution by gases from positive- ignition engines of motor vehicles. *Official Journal of the European Union*, L 32. Retrieved from <https://eur-lex.europa.eu/eli/dir/1977/102/oj>
- Parliament and Council of the European Union. (2007). Regulation (EC) No 715/2007 of the European Parliament and of the Council of 20 June 2007 on type approval of motor vehicles with respect to emissions from light passenger and commercial vehicles (Euro 5 and Euro 6) and on access to vehicle repair and maintenance information (Text with EEA relevance). *Official Journal of the European Union*, L 171. Retrieved from <http://data.europa.eu/eli/reg/2007/715/oj>
- European Commission & European Environment Agency (Eds.). (2013). *Environment and human health: Joint EEA-JRC report*. Luxembourg; Publ. Off. of the Europ. Union.

- Fenn, M. E., Bytnerowicz, A., Schilling, S. L., Vallano, D. M., Zavaleta, E. S., Weiss, S. B., ... Hanks, K. (2018). On-road emissions of ammonia: An underappreciated source of atmospheric nitrogen deposition. *Science of The Total Environment*, 625, 909–919. <https://doi.org/10.1016/j.scitotenv.2017.12.313>
- Giechaskiel, B., Isella, L., Colombo, R., Manfredi, U., Dilara, P., Drossinos, Y., ... De Santi, G. (2007). *Measurements in support of modelling the VELA-2 experimental facilities*. Retrieved from the European Commission Joint Research Centre website: http://publications.jrc.ec.europa.eu/repository/bitstream/JRC41981/report_vela2%20cvs%20modelling_final5.pdf
- Giechaskiel, B., Lähde, T., & Drossinos, Y. (2019). Regulating particle number measurements from the tailpipe of light-duty vehicles: The next step? *Environmental Research*, 172, 1–9. <https://doi.org/10.1016/j.envres.2019.02.006>
- Giechaskiel, B., Lähde, T., Suarez-Bertoa, R., Clairotte, M., Grigoratos, T., Zardini, A. A., ... Martini, G. (2018). Particle number measurements in the European legislation and future JRC activities. *Combustion Engines*, 3. http://www.combustion-engines.eu/entityfiles/files/articles_published/2018-301.pdf
- Giechaskiel, B., Manfredi, U., & Martini, G. (2014). Engine exhaust solid sub-23 nm particles: I. Literature survey. *SAE International Journal of Fuels and Lubricants*, 7(3), 950–964. <https://doi.org/10.4271/2014-01-2834>
- Giechaskiel, B., Maricq, M., Ntziachristos, L., Dardiotis, C., Wang, X., Axmann, H., ... Schindler, W. (2014). Review of motor vehicle particulate emissions sampling and measurement: From smoke and filter mass to particle number. *Journal of Aerosol Science*, 67, 48–86. <https://doi.org/10.1016/j.jaerosci.2013.09.003>
- Giechaskiel, B., Vanhanen, J., Väkevä, M., & Martini, G. (2017). Investigation of vehicle exhaust sub-23 nm particle emissions. *Aerosol Science and Technology*, 51(5), 626–641. <https://doi.org/10.1080/02786826.2017.1286291>
- Graham, L. A., Belisle, S. L., & Baas, C.-L. (2008). Emissions from light duty gasoline vehicles operating on low blend ethanol gasoline and E85. *Atmospheric Environment*, 42(19), 4498–4516. <https://doi.org/10.1016/j.atmosenv.2008.01.061>
- Graham, L. A., Belisle, S. L., & Rieger, P. (2009). Nitrous oxide emissions from light duty vehicles. *Atmospheric Environment*, 43(12), 2031–2044. <https://doi.org/10.1016/j.atmosenv.2009.01.002>
- Haagen-Smit, A. J. (1952). Chemistry and physiology of Los Angeles smog. *Industrial & Engineering Chemistry*, 44(6), 1342–1346. <https://doi.org/10.1021/ie50510a045>
- Hedge, M., Weber, P., Gingrich, J., Alger, T., & Khalek, I. A. (2011). Effect of EGR on particle emissions from a GDI engine. *SAE International Journal of Engines*, 4(1), 650–666. <https://doi.org/10.4271/2011-01-0636>
- Huai, T., Durbin, T. D., Wayne Miller, J., & Norbeck, J. M. (2004). Estimates of the emission rates of nitrous oxide from light-duty vehicles using different chassis dynamometer test cycles. *Atmospheric Environment*, 38(38), 6621–6629. <https://doi.org/10.1016/j.atmosenv.2004.07.007>
- Intergovernmental Panel on Climate Change. (2013). *Climate change 2013: The physical science basis. Contribution of Working Group I to the Fifth Assessment Report of the Intergovernmental Panel on Climate Change* (p. 1535). Cambridge University Press. Retrieved from <https://www.ipcc.ch/report/ar5/wg1/>
- Jin, D., Choi, K., Myung, C.-L., Lim, Y., Lee, J., & Park, S. (2017). The impact of various ethanol-gasoline blends on particulates and unregulated gaseous emissions characteristics from a spark ignition direct injection (SIDI) passenger vehicle. *Fuel*, 209, 702–712. <https://doi.org/10.1016/j.fuel.2017.08.063>

- Kar, K., & Cheng, W. K. (2009). *Speciated engine-out organic gas emissions from a PFI-SI engine operating on ethanol/gasoline mixtures* (SAE Technical Paper No. 2009-01-2673). Retrieved from the SAE International website: <http://papers.sae.org/2009-01-2673/>
- Kean, A. J., Littlejohn, D., Ban-Weiss, G. A., Harley, R. A., Kirchstetter, T. W., & Lunden, M. M. (2009). Trends in on-road vehicle emissions of ammonia. *Atmospheric Environment*, 43(8), 1565-1570. <https://doi.org/10.1016/j.atmosenv.2008.09.085>
- Khalek, I. A. (2019, January). *Particle Emissions from Gasoline Vehicles*. Presented at the Motor Vehicle/Vessel Emissions Control Workshop, Chengdu, China. Retrieved from <https://www.move2019.org/assets/doc/presentation/11%20D1%20E6%B1%BD%E6%B2%B9%E8%BD%A6%E9%A2%97%E7%B2%92%E7%89%A9%E6%8E%92%E6%94%BE-Imad%20Khalek.pdf>
- Link, M. F., Kim, J., Park, G., Lee, T., Park, T., Babar, Z. B., ... Farmer, D. K. (2017). Elevated production of NH₄NO₃ from the photochemical processing of vehicle exhaust: Implications for air quality in the Seoul Metropolitan Region. *Atmospheric Environment*, 156, 95-101. <https://doi.org/10.1016/j.atmosenv.2017.02.031>
- Livingston, C., Rieger, P., & Winer, A. (2009). Ammonia emissions from a representative in-use fleet of light and medium-duty vehicles in the California South Coast Air Basin. *Atmospheric Environment*, 43(21), 3326-3333. <https://doi.org/10.1016/j.atmosenv.2009.04.009>
- LoPachin, R. M., & Gavin, T. (2014). Molecular mechanisms of aldehyde toxicity: A chemical perspective. *Chemical Research in Toxicology*, 27(7), 1081-1091. <https://doi.org/10.1021/tx5001046>
- Manzetti, S., & Andersen, O. (2015). A review of emission products from bioethanol and its blends with gasoline. Background for new guidelines for emission control. *Fuel*, 140, 293-301. <https://doi.org/10.1016/j.fuel.2014.09.101>
- Momenimovahed, A., Handford, D., Checkel, M. D., & Olfert, J. S. (2015). Particle number emission factors and volatile fraction of particles emitted from on-road gasoline direct injection passenger vehicles. *Atmospheric Environment*, 102, 105-111. <https://doi.org/10.1016/j.atmosenv.2014.11.045>
- Nevalainen, P., Kinnunen, N. M., Kirveslahti, A., Kallinen, K., Maunula, T., Keenan, M., & Suvanto, M. (2018). Formation of NH₃ and N₂O in a modern natural gas three-way catalyst designed for heavy-duty vehicles: The effects of simulated exhaust gas composition and ageing. *Applied Catalysis A: General*, 552, 30-37. <https://doi.org/10.1016/j.apcata.2017.12.017>
- Ntziachristos, L., Kontses, A., Toumasatos, Z., Triantafyllopoulos, G., Kolokotronis, D., & Samaras, Z. (2019, January). *Gaseous and Particulate pollutant measurements on the road and in the lab from latest car technologies in Europe*. Presented at the Motor Vehicle/Vessel Emissions Control Workshop, Chengdu, China. Retrieved from https://www.move2019.org/assets/doc/presentation/6%20D2A%20Ntziachristos_Emissions.pdf
- Parliament and Council of the European Union. (1996). Directive 96/69/EC of the European Parliament and of the Council of 8 October 1996 amending Directive 70/220/EEC on the approximation of the laws of the Member States relating to measures to be taken against air pollution by emissions from motor vehicles. *Official Journal of the European Union*, L 282. Retrieved from <https://eur-lex.europa.eu/eli/dir/1996/69/oj>

- Parliament and Council of the European Union. (1998). Directive 98/69/EC of the European Parliament and of the Council of 13 October 1998 relating to measures to be taken against air pollution by emissions from motor vehicles and amending Council Directive 70/220/EEC. *Official Journal of the European Union*, L 350. Retrieved from <https://eur-lex.europa.eu/eli/dir/1998/69/oj>
- Pavlovic, J., Marotta, A., & Ciuffo, B. (2016). CO₂ emissions and energy demands of vehicles tested under the NEDC and the new WLTP type approval test procedures. *Applied Energy*, 177, 661–670. <https://doi.org/10.1016/j.apenergy.2016.05.110>
- Pfau, S. A., La Rocca, A., Haffner-Staton, E., Rance, G. A., Fay, M. W., Brough, R. J., & Malizia, S. (2018). Comparative nanostructure analysis of gasoline turbocharged direct injection and diesel soot-in-oil with carbon black. *Carbon*, 139, 342–352. <https://doi.org/10.1016/j.carbon.2018.06.050>
- Platt, S. M., Haddad, I. E., Pieber, S. M., Zardini, A. A., Suarez-Bertoa, R., Clairotte, M., ... Prévôt, A. S. H. (2017). Gasoline cars produce more carbonaceous particulate matter than modern filter-equipped diesel cars. *Scientific Reports*, 7(1), 4926. <https://doi.org/10.1038/s41598-017-03714-9>
- Raj, A. (2016). Methane emission control. *Johnson Matthey Technology Review*, 60(4), 228–235. <https://doi.org/10.1595/205651316X692554>
- Raza, M., Chen, L., Leach, F., & Ding, S. (2018). A review of particulate number (PN) emissions from gasoline direct injection (GDI) engines and their control techniques. *Energies*, 11(6), 1417. <https://doi.org/10.3390/en11061417>
- Rodríguez, J. F. (2016). *Investigations on the pollutant emissions of gasoline direct injection engines during cold-start* (Doctoral thesis.) Massachusetts Institute of Technology. Retrieved from <http://dspace.mit.edu/handle/1721.1/104130>
- Suarez-Bertoa, R., & Astorga, C. (2016a). Isocyanic acid and ammonia in vehicle emissions. *Transportation Research Part D: Transport and Environment*, 49, 259–270. <https://doi.org/10.1016/j.trd.2016.08.039>
- Suarez-Bertoa, R., & Astorga, C. (2016b). Unregulated emissions from light-duty hybrid electric vehicles. *Atmospheric Environment*, 136, 134–143. <https://doi.org/10.1016/j.atmosenv.2016.04.021>
- Suarez-Bertoa, R., & Astorga, C. (2018). Impact of cold temperature on Euro 6 passenger car emissions. *Environmental Pollution*, 234, 318–329. <https://doi.org/10.1016/j.envpol.2017.10.096>
- Suarez-Bertoa, R., Mendoza-Villafuerte, P., Riccobono, F., Vojtisek, M., Pechout, M., Perujo, A., & Astorga, C. (2017). On-road measurement of NH₃ emissions from gasoline and diesel passenger cars during real world driving conditions. *Atmospheric Environment*, 166, 488–497. <https://doi.org/10.1016/j.atmosenv.2017.07.056>
- Suarez-Bertoa, R., Zardini, A. A., & Astorga, C. (2014). Ammonia exhaust emissions from spark ignition vehicles over the New European Driving Cycle. *Atmospheric Environment*, 97, 43–53. <https://doi.org/10.1016/j.atmosenv.2014.07.050>
- Suarez-Bertoa, R., Zardini, A. A., Lilova, V., Meyer, D., Nakatani, S., Hibel, F., ... Astorga, C. (2015). Intercomparison of real-time tailpipe ammonia measurements from vehicles tested over the new world-harmonized light-duty vehicle test cycle (WLTC). *Environmental Science and Pollution Research*, 22(10), 7450–7460. <https://doi.org/10.1007/s11356-015-4267-3>
- Sun, K., Tao, L., Miller, D. J., Pan, D., Golston, L. M., Zondlo, M. A., ... Zhu, T. (2017). Vehicle emissions as an important urban ammonia source in the United States and China. *Environmental Science & Technology*, 51(4), 2472–2481. <https://doi.org/10.1021/acs.est.6b02805>

- Tsiakmakis, S., Fontaras, G., Ciuffo, B., & Samaras, Z. (2017). A simulation-based methodology for quantifying European passenger car fleet CO₂ emissions. *Applied Energy*, 199, 447–465. <https://doi.org/10.1016/j.apenergy.2017.04.045>
- United Nations Economic Commission for Europe. (2015). *Regulation No. 83, Revision 5. Uniform provisions concerning the approval of vehicles with regard to the emission of pollutants according to engine fuel requirements* (No. E/ECE/324/Rev.1/Add.82/Rev.5–E/ECE/TRANS/505/Rev.1/Add.82/Rev.5). Retrieved from <https://www.unece.org/fileadmin/DAM/trans/main/wp29/wp29regs/R083r5e.pdf>
- U.S. Environmental Protection Agency. (2014a). *Control of air pollution from motor vehicles: Tier 3 motor vehicle emission and fuel standards; Final rule* [Federal Register / Vol. 79, No. 81]. Retrieved from <https://www.govinfo.gov/content/pkg/FR-2014-04-28/pdf/2014-06954.pdf>
- U.S. Environmental Protection Agency. (2014b, September 15). Particle pollution exposure [Collections and lists]. Retrieved February 21, 2019, from <https://www.epa.gov/pmcourse/particle-pollution-exposure>
- Walsh, M. P. (2003). Vehicle emissions and health in developing countries. In McGranhan, G., & Murray, F. (Eds.), *Air pollution and health in rapidly developing countries* (pp. 174–203). Retrieved from <https://content.taylorfrancis.com/books/e/download?dac=C2011-0-07202-6&isbn=9781136571848&doi=10.4324/9781849770460-17&format=pdf>
- Winer, A. M., & Behrentz, E. (2005). *Estimates of nitrous oxide emissions from motor vehicles and the effects of catalyst composition and aging*. Retrieved from the California Air Resources Board website: <https://www.arb.ca.gov/research/apr/past/02-313.pdf>
- World Health Organization. (2016). *Ambient air pollution: A global assessment of exposure and burden of disease*. Retrieved from <http://www.who.int/phe/publications/air-pollution-global-assessment/en/>
- Xue, J., Li, Y., Wang, X., Durbin, T. D., Johnson, K. C., Karavalakis, G., ... Jung, H. S. (2015). Comparison of vehicle exhaust particle size distributions measured by SMPS and EEPS during steady-state conditions. *Aerosol Science and Technology*, 49(10), 984–996. <https://doi.org/10.1080/02786826.2015.1088146>

APPENDIX: TABULATED EMISSIONS

Table A1. Bag emission factors over the tested cycles for the regulated pollutants

Cycle	Temp.	Start	NO _x (mg/km)	PN (# 10 ¹¹ /km)	NMHC (mg/km)	CO (mg/km)
NEDC	23°C	Cold	17.2 ± 1.6	1.10 ± 0.04	23.2 ± 2.8	157 ± 25
	23°C	Hot	5.9 ± 1.4	0.58 ± 0.24	2.3 ± 1.2	23 ± 7
	23°C	Hot, high load ^a	6.1 ± 0.6	0.67 ± 0.13	2.8 ± 0.2	37 ± 6
	10°C	Cold	18.0 ± 0.2	3.39 ± 0.51	26.8 ± 0.4	163 ± 10
WLTC	23°C	Cold	13.6 ± 0.4	1.46 ± 0.06	11.4 ± 1.4	91 ± 6
	23°C	Hot	8.3 ± 2.1	0.90 ± 0.16	1.1 ± 0.4	50 ± 22
	14°C	Cold	13.2 ± 1.7	2.44 ± 0.08	13.1 ± 0.9	116 ± 26
RDC	23°C	Cold	9.3 ± 1.2	2.26 ± 0.11	12.6 ± 1.4	159 ± 20
	23°C	Hot	6.5 ± 0.5	1.21 ± 0.12	3.6 ± 0.3	85 ± 20
	-7°C	Cold ^b	16.9	13.68	65.4	336
RDC-City	23°C	Cold	12.4 ± 3.6	3.38 ± 0.74	14.4 ± 0.3	200 ± 7
	23°C	Hot	9.0 ± 1.6	1.31 ± 0.21	3.2 ± 0.0	130 ± 7
	-7°C	Cold ^b	28.0	16.97	78.0	389
	-7°C	Hot ^a	5.7	1.89	2.8	40

Note: The average and maximum error are shown.

^aDuring these tests, the air conditioning was operated at the lowest temperature and the highest fan speed. Additionally, the vehicles lights were on.

^bOnly one valid run was recorded

Table A2. Emission factors over the NEDC and WLTC for solid PN with 23 nm and 10 nm counting thresholds

Cycle	Temp.	Start	PN (>23 nm) (# 10 ¹¹ /km)	PN (>10 nm) (# 10 ¹¹ /km)
NEDC	23°C	Cold	1.10 ± 0.04	1.77 ± 0.03
	23°C	Hot	0.59 ± 0.03	0.89 ± 0.03
	23°C	Hot, high load ^a	0.67 ± 0.13	1.22 ± 0.06
	10°C	Cold ^b	3.39 ± 0.51	4.26 ± 0.62
WLTC	23°C	Cold ^c	1.39	2.04
	23°C	Hot ^c	1.07	1.56
	14°C	Cold	2.44 ± 0.08	3.2 ± 0.06

Note: The average and maximum error are shown.

^aDuring these tests, the air conditioning was operated at the lowest temperature and the highest fan speed. Additionally, the vehicles lights were on.

^bNo valid CPC measurements for PN > 10 nm. Estimation from CPC > 23 nm and EEPS results.

^cOnly one valid run was recorded.

Table A3. Ammonia emission factors and average ammonia concentration over the NEDC, WLTC, RDC, and RDC-City tests

Cycle	Temp.	Start	NH ₃ (mg/km)	Avg. NH ₃ (ppm)
NEDC	23°C	Cold	3.3 ± 0.8	6.1 ± 1.2
	23°C	Hot	1.7 ± 0.1	4.9 ± 0.3
	23°C	Hot, high load ^a	5.8 ± 1.0	14.6 ± 3.0
	10°C	Cold	3.0 ± 1.8	5.9 ± 3.0
WLTC	23°C	Cold	3.2 ± 0.5	6.6 ± 0.5
	23°C	Hot	4.1 ± 1.5	7.7 ± 2.5
	14°C	Cold	2.7 ± 0.5	6.6 ± 1.3
RDC	23°C	Cold	6.0 ± 1.6	10.3 ± 4.0
	23°C	Hot ^b	7.1	9.8
	-7°C	Cold ^b	11.5	17.5
RDC-City	23°C	Cold	8.1 ± 0.9	11.6 ± 2.3
	23°C	Hot	4.8 ± 2.7	5.7 ± 1.9
	-7°C	Cold ^b	11.2	19.1
	-7°C	Hot ^b	6.7	6.3

Note: The average and maximum error are shown.

^aDuring these tests, the air conditioning was operated at the lowest temperature and the highest fan speed. Additionally, the vehicles lights were on.

^bOnly one valid run was recorded

Table A4. Methane and nitrous oxide emission factors, and their combined 20-year and 100-year CO₂ equivalence, over the NEDC, WLTC, RDC, and RDC-City tests

Cycle	Temp.	Start	CH ₄ (mg/km)	N ₂ O (mg/km)	CO ₂ -eq (20 year) (g/km)	CO ₂ -eq (100 year) (g/km)
NEDC	23°C	Cold	3.7 ± 0.5	1.5 ± 0.3	0.71 ± 0.10	0.23 ± 0.03
	23°C	Hot	2.3 ± 0.2	0.4 ± 0.1	0.29 ± 0.04	0.09 ± 0.01
	23°C	Hot, high load ^a	1.6 ± 0.1	1.4 ± 0.3	0.51 ± 0.08	0.18 ± 0.03
	10°C	Cold	4.9 ± 0.2	1.5 ± 0.2	0.80 ± 0.07	0.25 ± 0.02
WLTC	23°C	Cold	1.3 ± 0.2	0.5 ± 0.2	0.25 ± 0.03	0.08 ± 0.01
	23°C	Hot	0.8 ± 0.2	0.3 ± 0.1	0.14 ± 0.04	0.05 ± 0.01
	14°C	Cold	1.5 ± 0.1	0.7 ± 0.1	0.30 ± 0.04	0.10 ± 0.01
RDC	23°C	Cold	1.8 ± 0.2	0.4 ± 0.0	0.27 ± 0.02	0.08 ± 0.01
	23°C	Hot ^b	1.7	0.2	0.19	0.05
	-7°C	Cold ^b	4.8	0.9	0.64	0.20
RDC-City	23°C	Cold	2.3 ± 0.2	0.5 ± 0.1	0.33 ± 0.01	0.10 ± 0.01
	23°C	Hot	1.5 ± 0.2	0.2 ± 0.0	0.18 ± 0.02	0.05 ± 0.01
	-7°C	Cold ^b	5.5	1.3	0.82	0.25
	-7°C	Hot ^b	0.9	0.2	0.12	0.04

Note: The average and maximum error are shown.

^aDuring these tests, the air conditioning was operated at the lowest temperature and the highest fan speed. Additionally, the vehicles lights were on.

^bOnly one valid run was recorded

Table A5. Formaldehyde emission factors over the NEDC, WLTC, RDC, and RDC-City tests

Cycle	Temp.	Start	HCHO (mg/km)
NEDC	23°C	Cold	0.23 ± 0.5×10 ⁻²
	23°C	Hot	0.06 ± 0.9×10 ⁻²
	23°C	Hot, high load ^a	0.07 ± 1.8×10 ⁻²
	10°C	Cold	0.20 ± 0.9×10 ⁻²
WLTC	23°C	Cold	0.14 ± 1.9×10 ⁻²
	23°C	Hot	0.04 ± 1.1×10 ⁻²
	14°C	Cold	0.17 ± 0.4×10 ⁻²
RDC	23°C	Cold	0.07 ± 0.4×10 ⁻²
	23°C	Hot ^b	-
	-7°C	Cold ^c	0.12
RDC-City	23°C	Cold	0.09 ± 0.6×10 ⁻²
	23°C	Hot ^b	-
	-7°C	Cold ^c	0.14
	-7°C	Hot ^b	-

Note: The average and maximum error are shown.

^aDuring these tests, the air conditioning was operated at the lowest temperature and the highest fan speed. Additionally, the vehicles lights were on.

^bBelow the detection limit

^cOnly one valid run was recorded

Table A6. Range of unregulated emissions found in the literature

Pollutant	Range	Source
10 to 23 nm solid particle fraction	74 - 94%	(Giechaskiel et al., 2019)
	0 - 260%	(Ntziachristos et al., 2019)
	36 - 50%	(Giechaskiel et al., 2017)
Volatile to total particle fraction	0 - 49%	(Momenimovahed, Handford, Checkel, & Olfert, 2015)
	30 - 59%	(Xue et al., 2015)
	68 - 93%	(Hedge, Weber, Gingrich, Alger, & Khalek, 2011)
NH ₃	3 - 25 mg/km	(Suarez-Bertoa et al., 2017)
	6 - 55 mg/km	(Suarez-Bertoa & Astorga, 2016a)
	4 - 70 mg/km	(Suarez-Bertoa et al., 2014)
N ₂ O	0.7 - 3.7 mg/km	(Chan et al., 2013)
	4 - 64 mg/km	(Behrentz et al., 2004)
	4.3 - 43 mg/km	(Huai, Durbin, Wayne Miller, & Norbeck, 2004)
CH ₄	0.7 - 3.8 mg/km	(Suarez-Bertoa & Astorga, 2016b)
	3.1 - 36 mg/km	(Chan et al., 2013)
HCHO	0.3 - 1.3 mg/km	(Jin et al., 2017), Fuel: E85
	0.4 - 0.7 mg/km	(Suarez-Bertoa et al., 2015), Fuel: E5
	0 - 0.8 mg/km	(Graham, Belisle, & Baas, 2008), Fuel: E20